Lecture 21 B. The variable-phase model

- enables treatment of weakly nonresonant effects arising in multiple particle interactions

PhD of Miles M. P. Couchman

Droplet-droplet interactions

- multiple droplets interact at a distance through shared wavefield
- interaction can be attractive or repulsive according to gradient of local wavefield
- variety of bound states may be formed
  - inter-drop distances are quantized: drops bounce in minima of wavefield generated by neighbors

Bound droplet pairs

Couder *et al.* 2005; Protière *et al*. 2006, 2008; Eddi *et al.* 2008; Borghesi *et al*. 2014; Oza *et al*. 2017; Arbelaiz *et al*. 2018

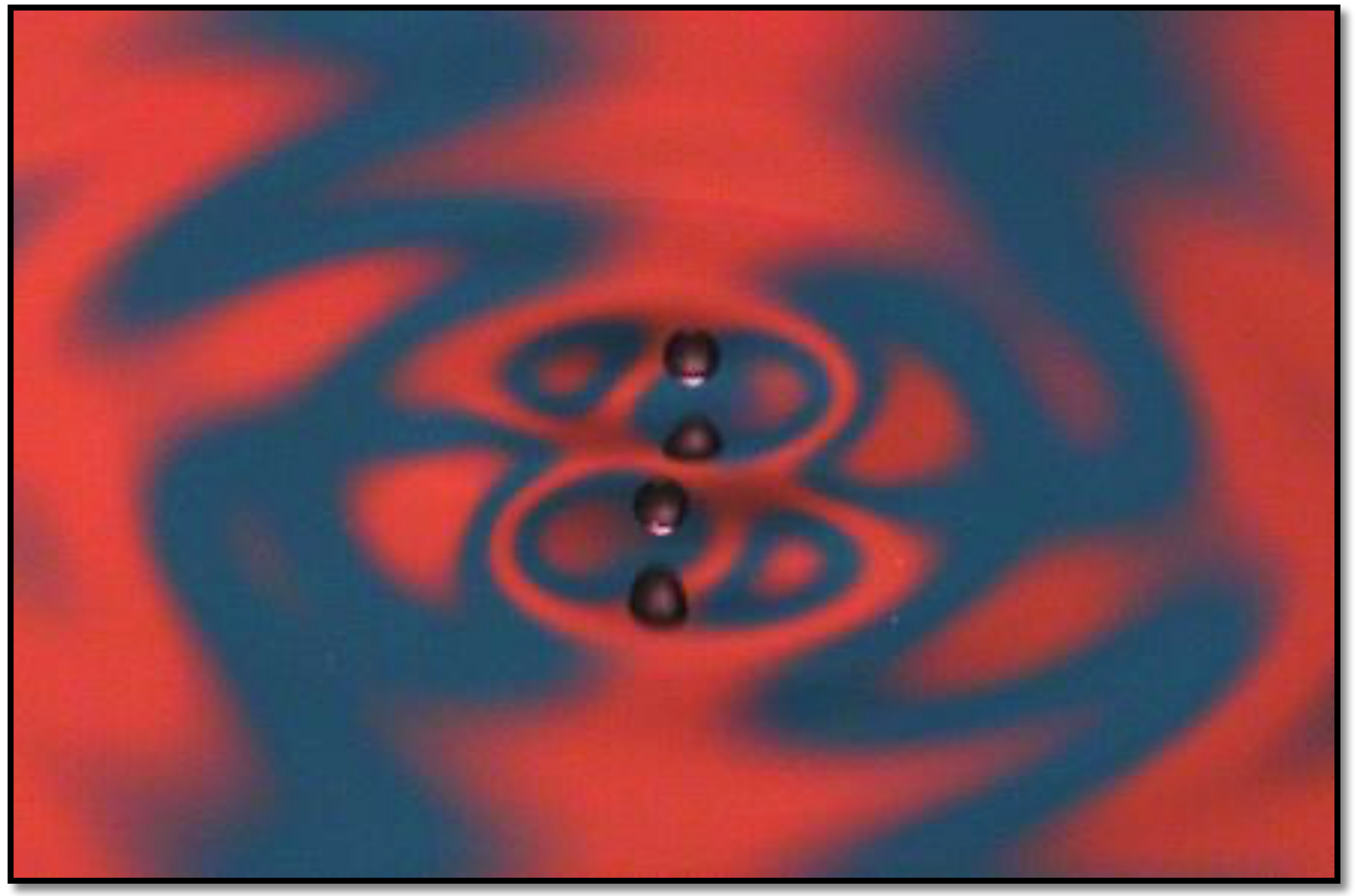

Droplet lattices

Protière *et al*. 2005; Lieber *et al.* 2007; Eddi *et al.* 2008, 2009, 2011

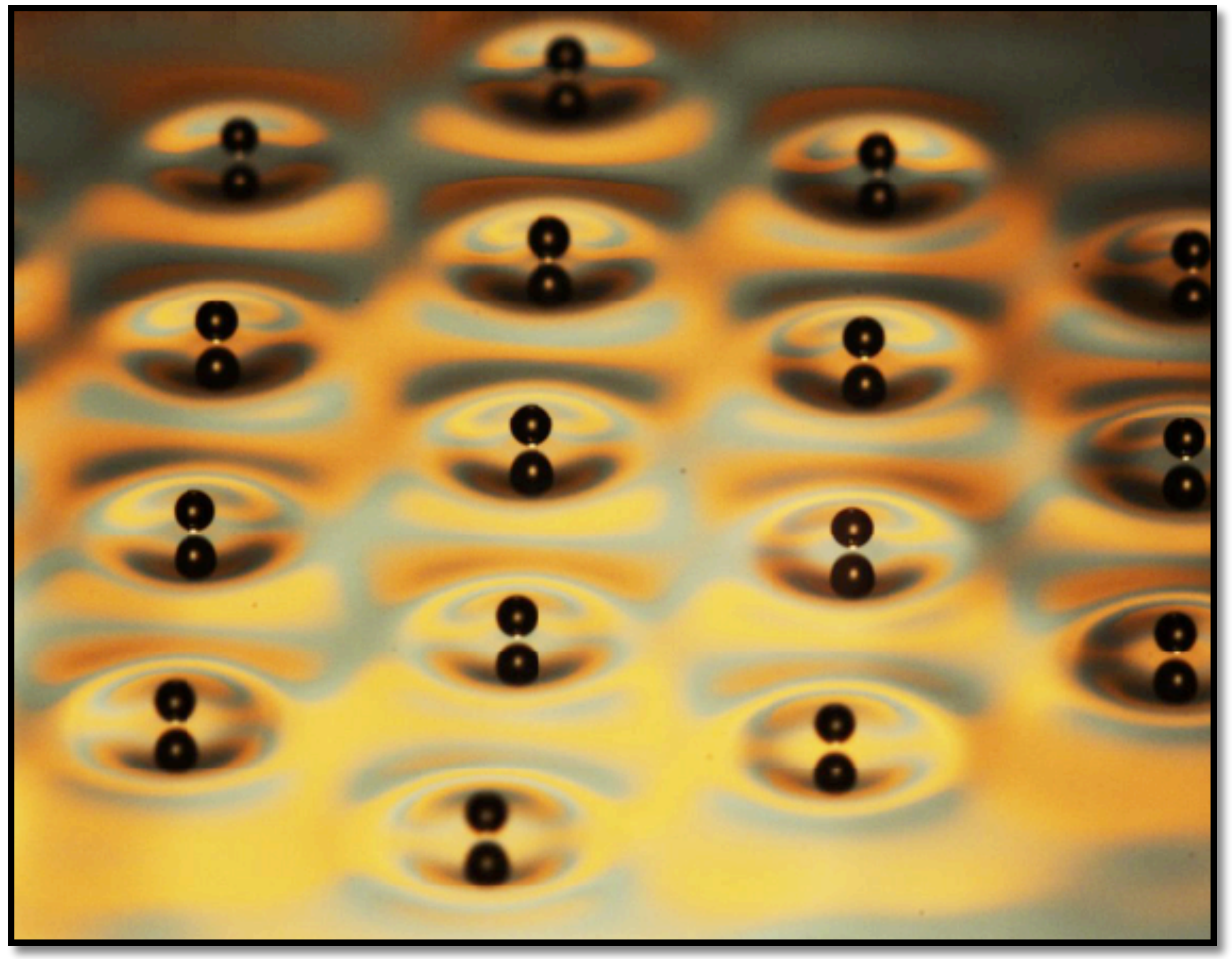

Theoretical models

Theoretical models for walking droplets split into two classes

(see review article: S.E. Turton, **M.M.P. Couchman**, and J.W.M. Bush, *Chaos* 2018)

Full treatment of drop's coupled vertical and horizontal motion

(Moláček and Bush 2013; Milewski *et al.* 2015; C.A. Galeano-Rios *et al.* 2017, 2019)

- Large separation of timescales between vertical and horizontal motion
  - Computationally expensive
- Unamenable to stability analysis

Simulation/real time:
$10^2 - 10^4$

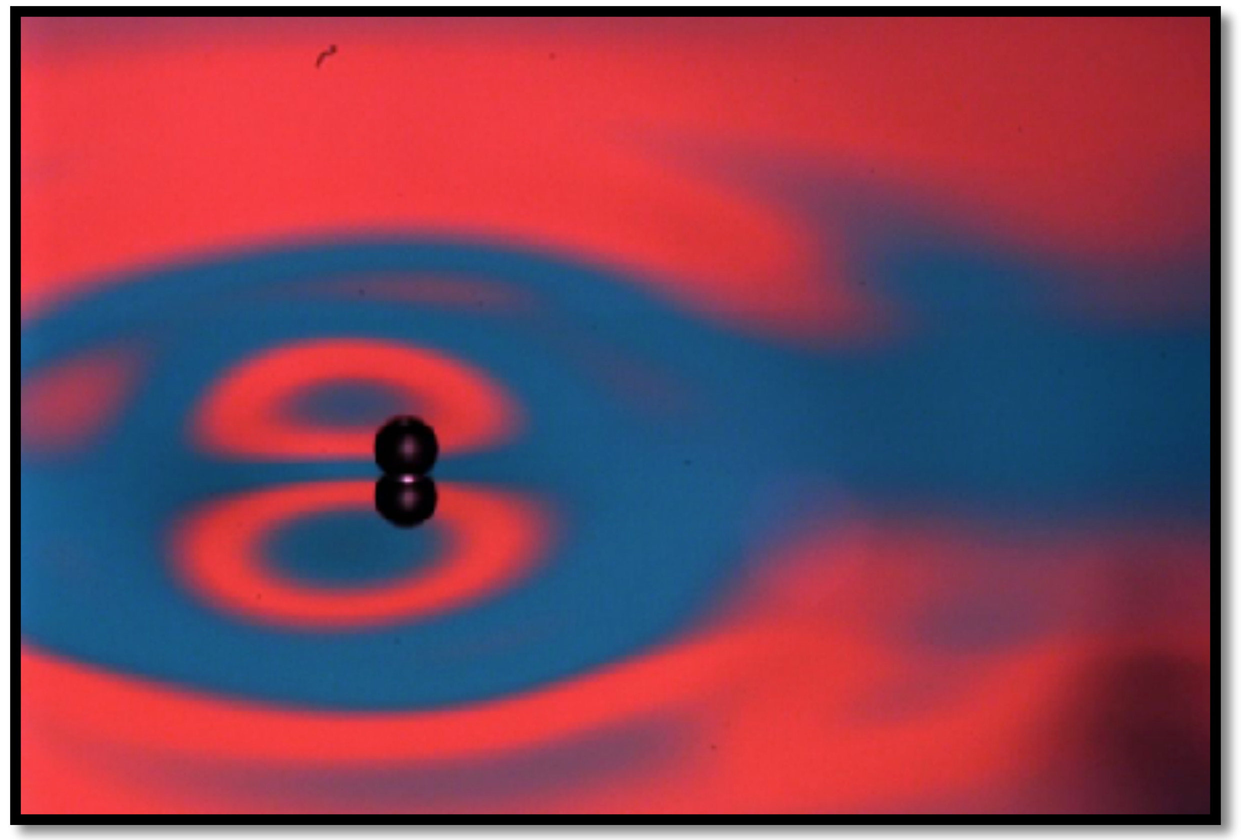

Fixed, periodic vertical motion assumed

(Fort *et al.* 2010; Oza *et al.* 2013; Bush *et al.* 2014; Labousse and Perrard 2014; Dubertrand *et al.* 2016; Faria 2017; Nachbin *et al.* 2017; Durey and Milewski 2017)

- 'Stroboscopic approximation' (Oza *et al.* 2013)
  - Time-average over drop's bouncing period
  - Information about vertical dynamics contained within unspecified phase parameter $\sin\Phi$

Simulation/real time:
$10^{-3} - 10^0$

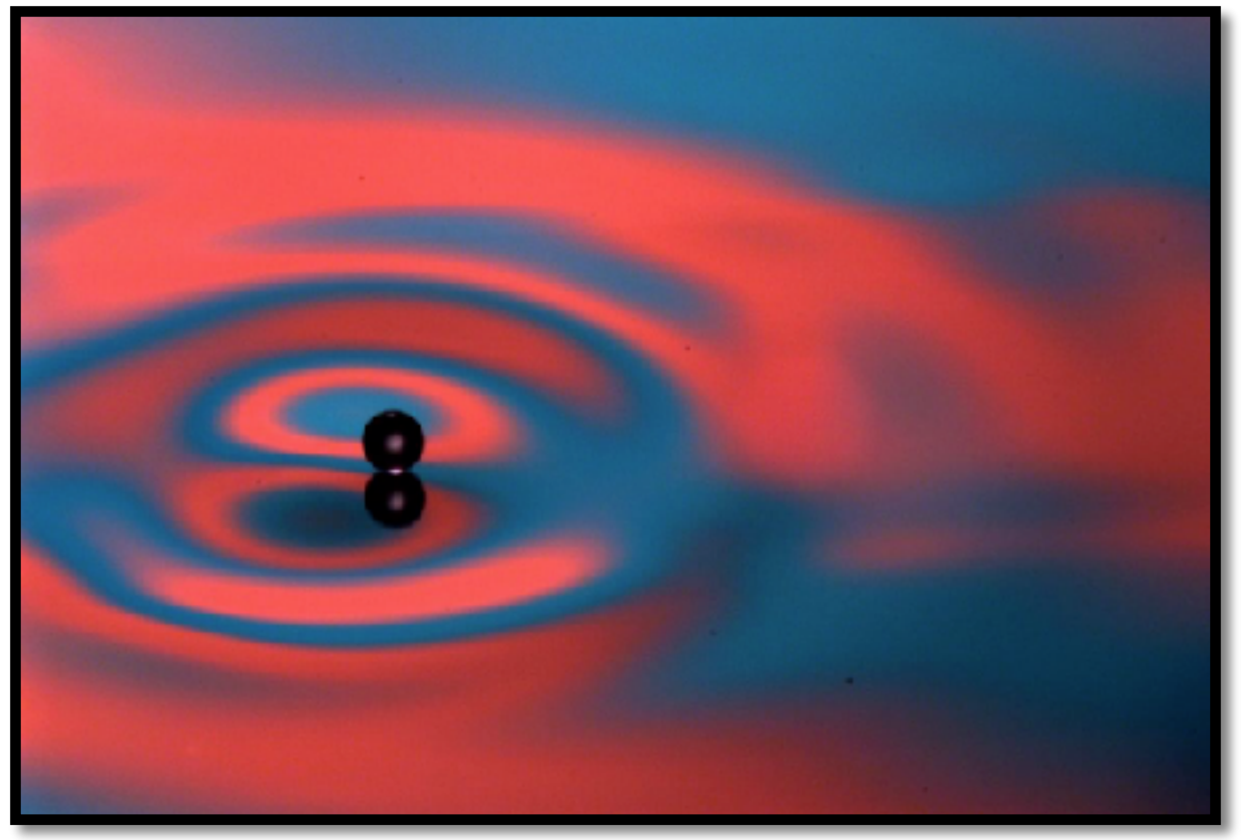

Limitations of stroboscopic approximation

- limited predictive power
  - Phase parameter varies between studies: $\sin\Phi \in (0.16 - 0.5)$
- shortcomings in predicting stability of single drop orbital motion in central force or rotating frame
  (Oza *et al*. 2014; Labousse *et al*. 2016)
- variations in vertical dynamics found to have significant influence on droplet-droplet interactions
  - orbiting, promenading, ratcheting pairs
    (Oza *et al*. 2017; Arbelaiz *et al*. 2018; Galeano-Rio et al. 2018)
  - droplet-droplet scattering events
    (Tadrist *et al*. 2018)

Quantized orbital radii in rotating frame

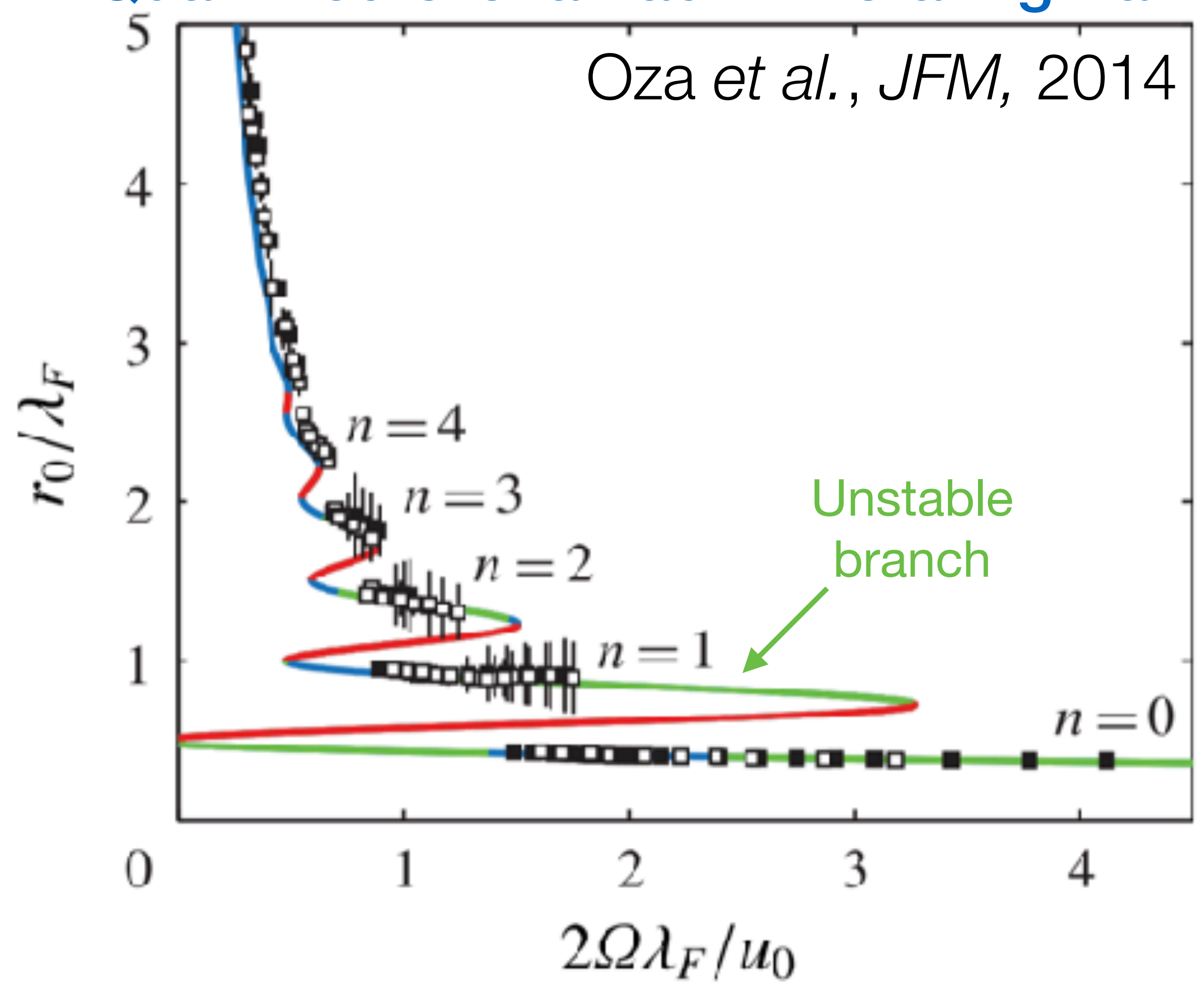

Orbiting pair

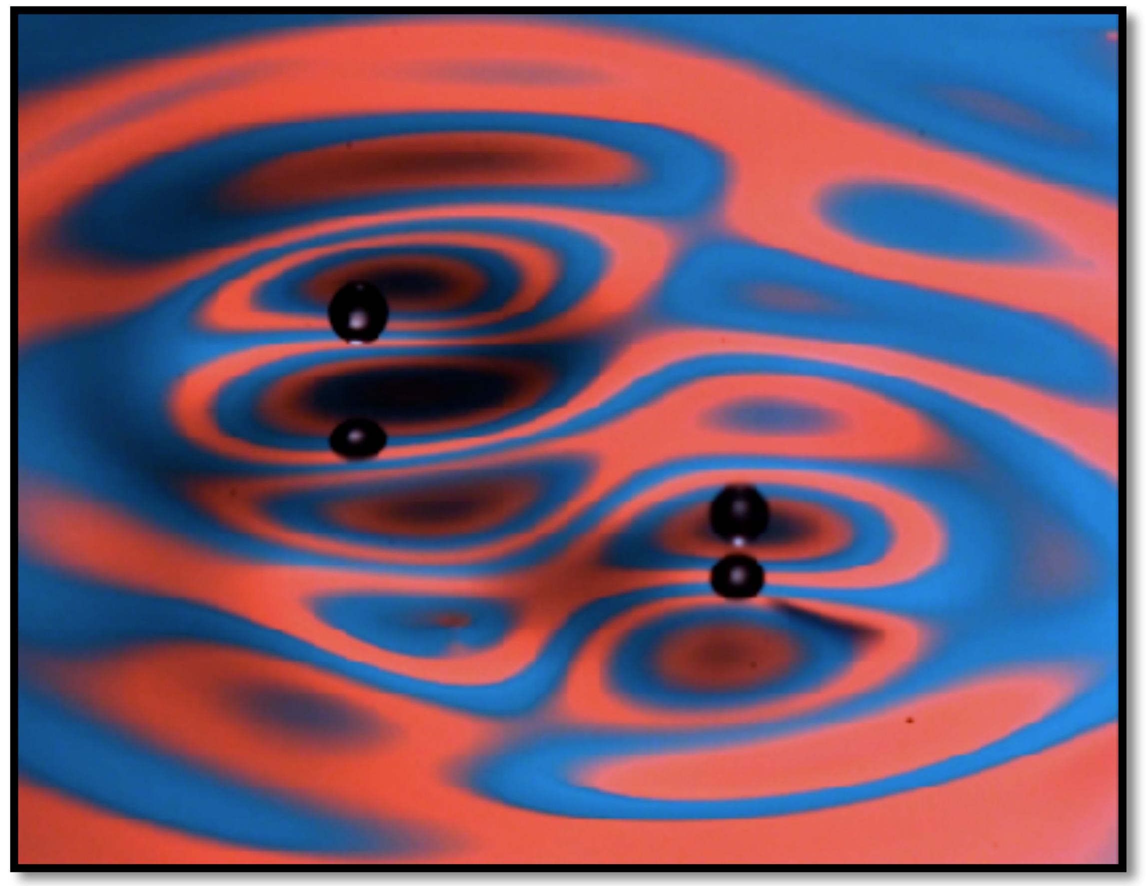

Promenading pair

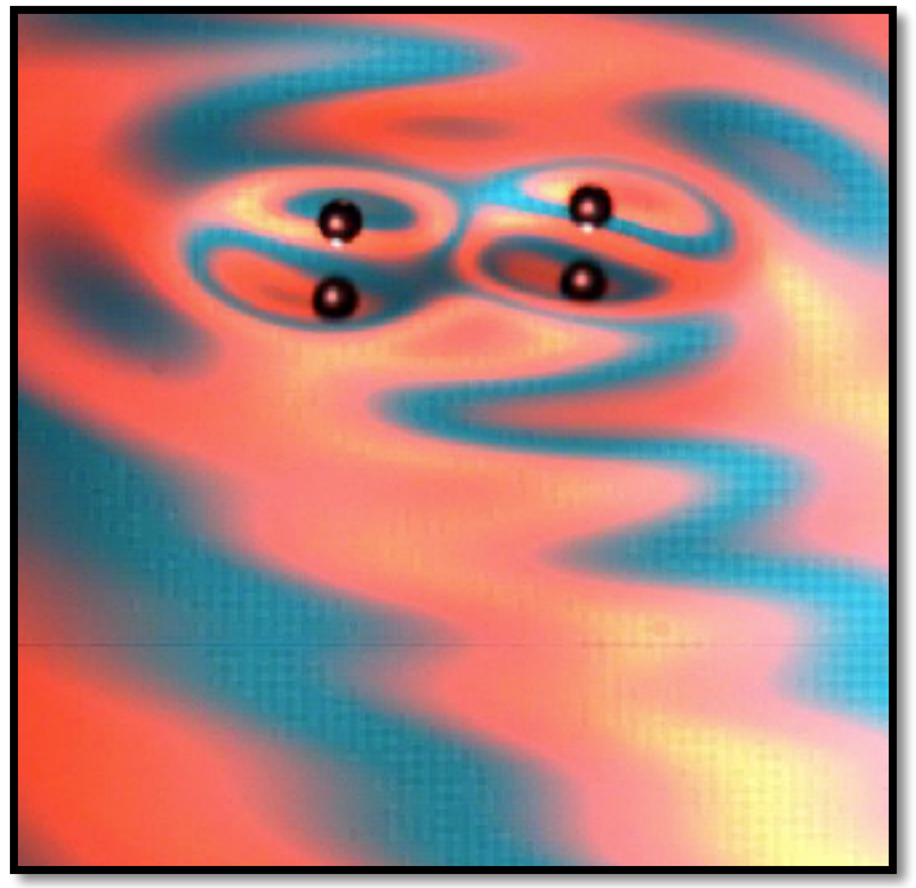

Objectives

- develop analytically tractable trajectory equation that accounts for variations in vertical dynamics
- characterize how modulations in vertical dynamics affect stability of bound droplet aggregates

Experiments and linear stability analysis

Model for coupling of vertical and horizontal motion

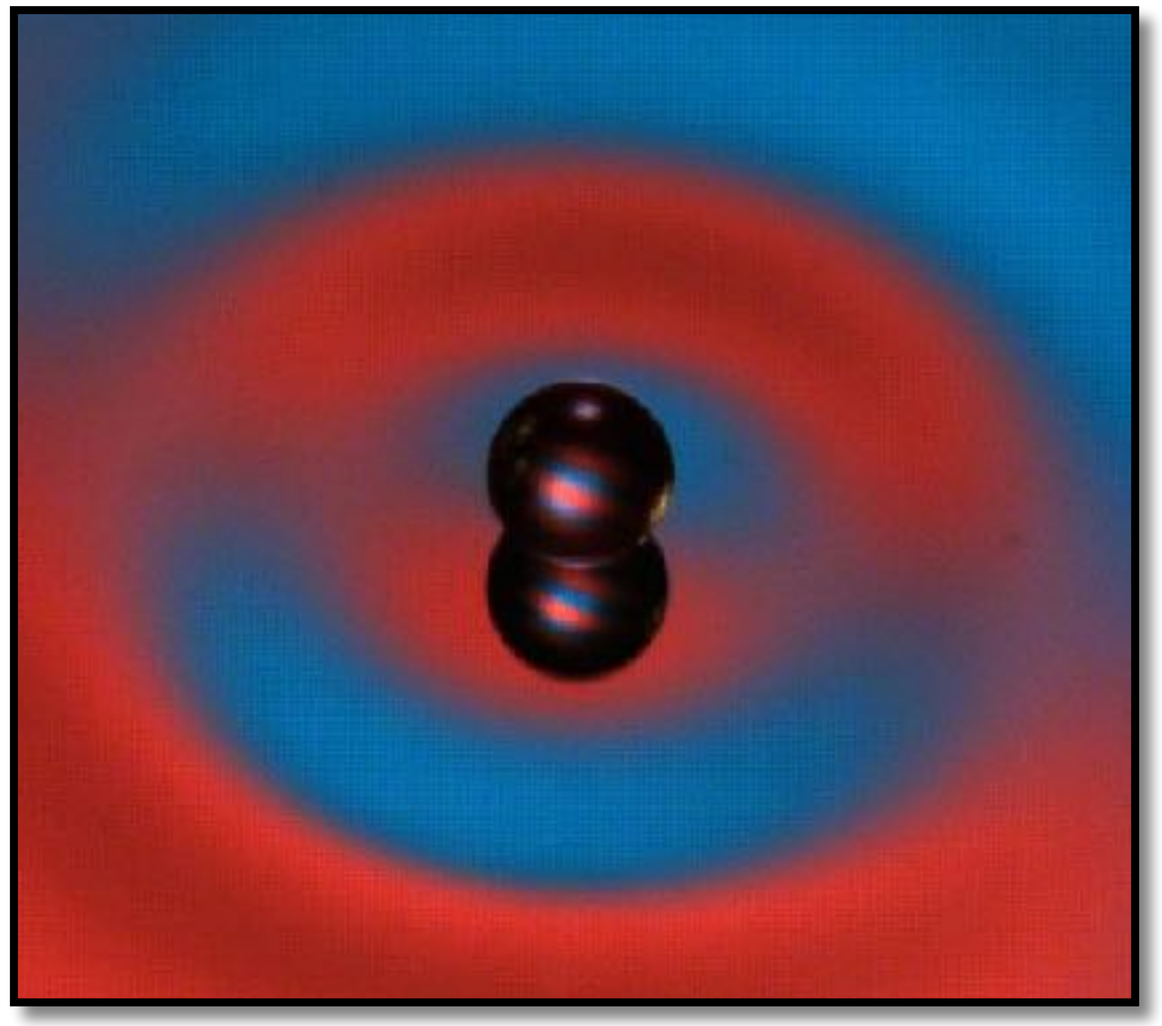

Pairs

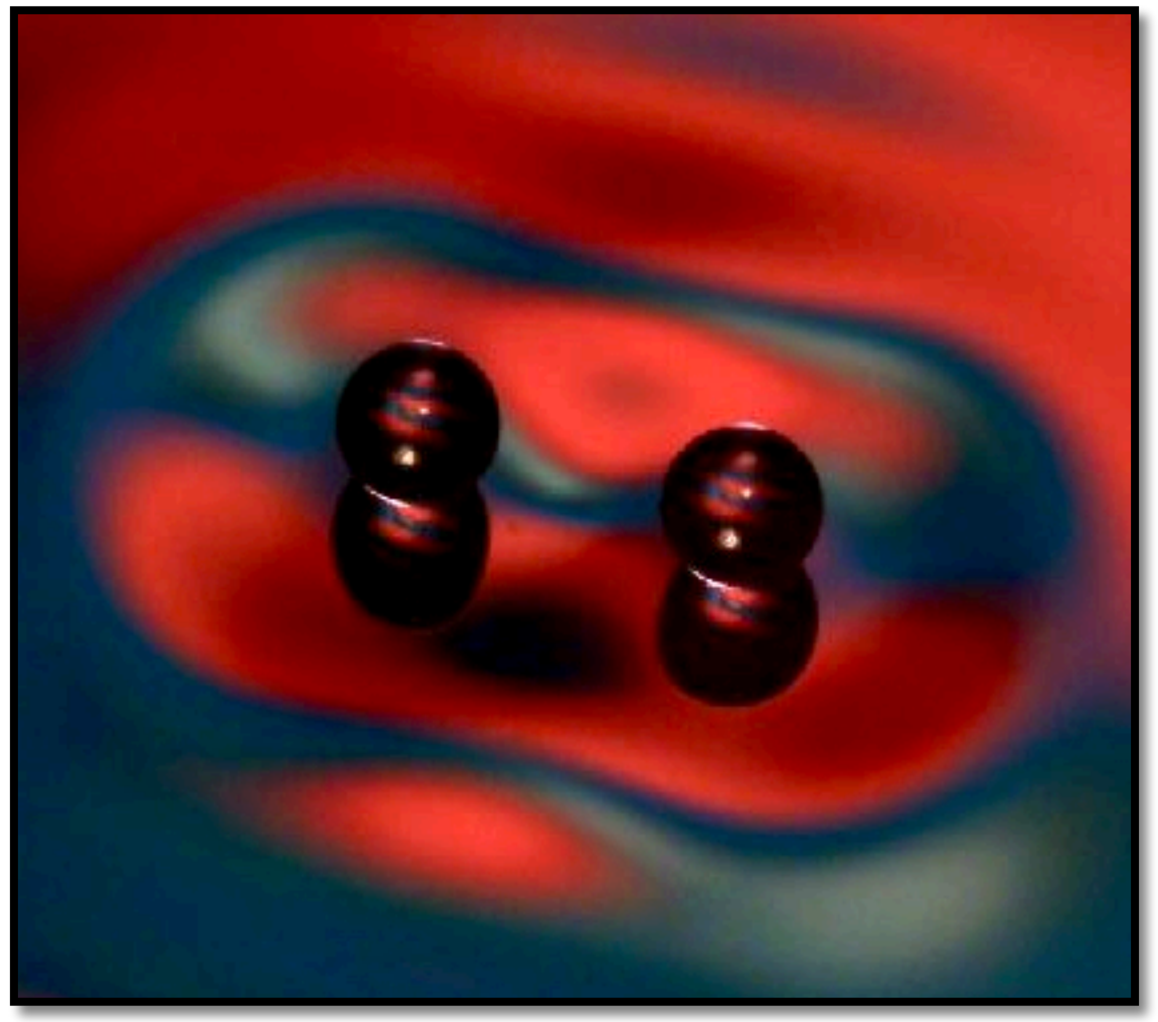

Rings

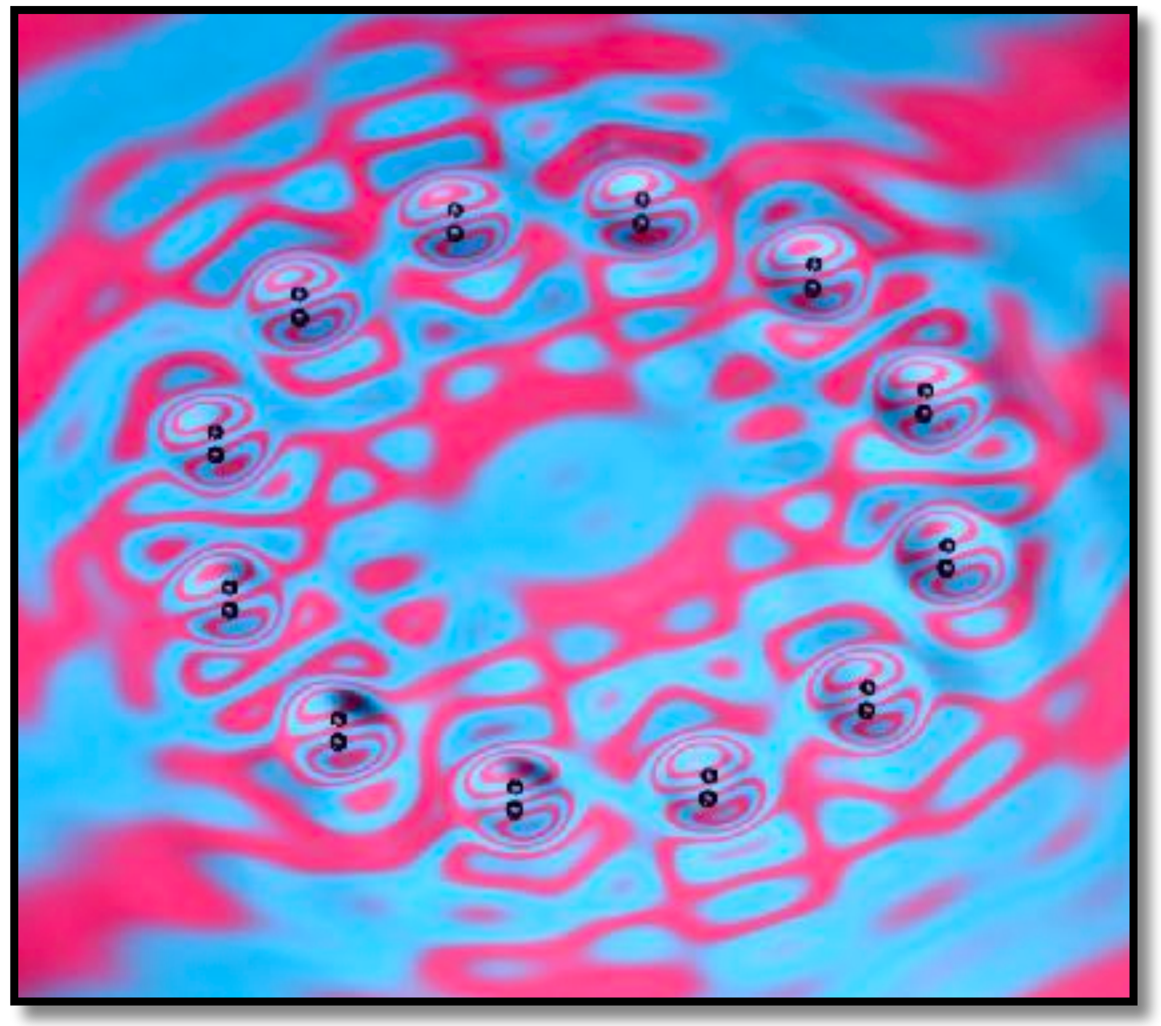

Conclusions and future work

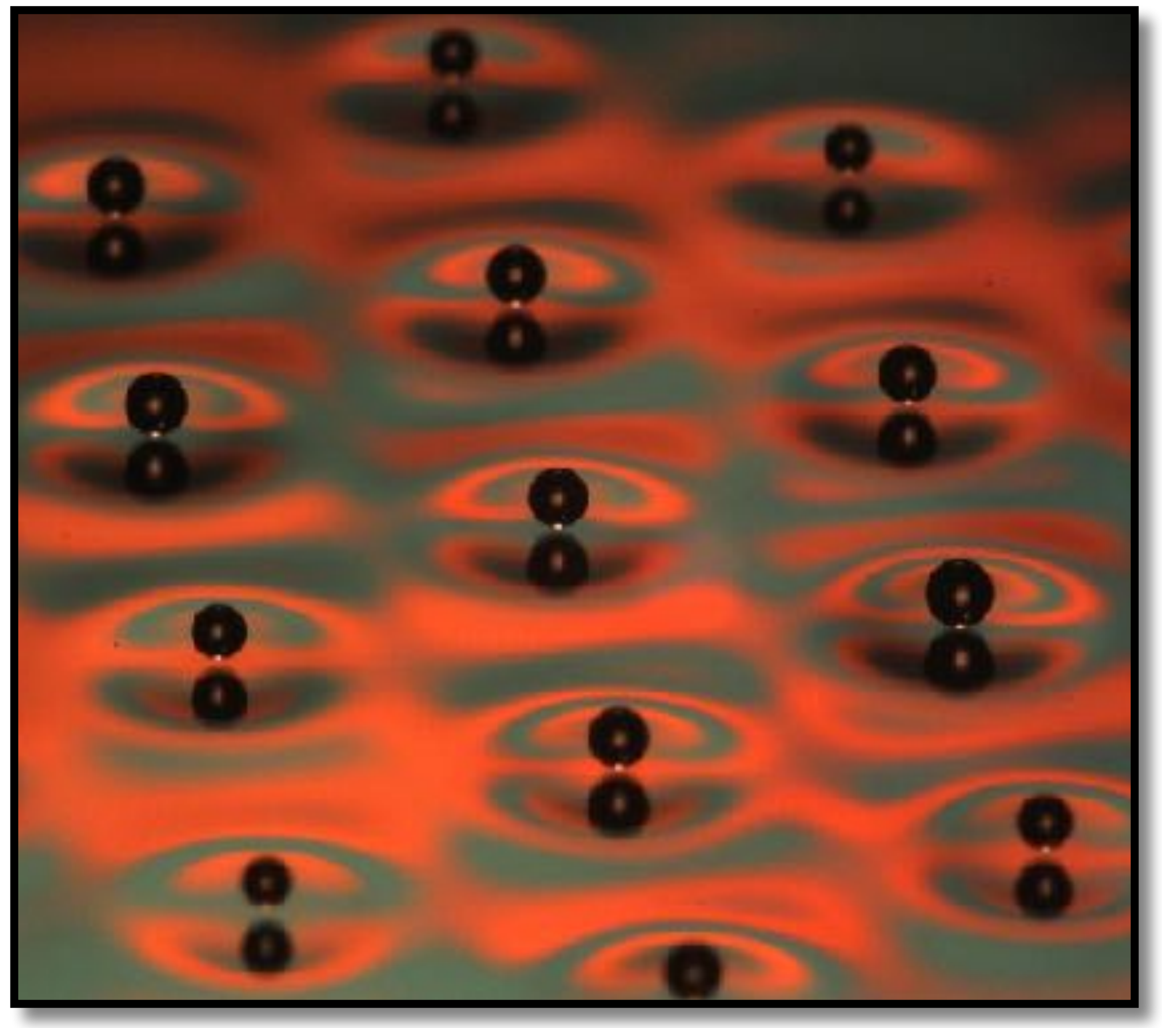

Contributions:

- **M.M.P. Couchman** and J.W.M. Bush. Free rings of bouncing droplets: stability and dynamics. *Under review at JFM.*
- **M.M.P. Couchman**, S.E. Turton, and J.W.M. Bush. Bouncing phase variations in pilot-wave hydrodynamics and the stability of droplet pairs. *JFM* (2019)
- **M.M.P. Couchman**, S.J. Thomson, and J.W.M. Bush. Pilot-wave theory: a mathematical bridge. *Finalist and Honorable Mention — NSF We Are Mathematics Video Competition* (2019)
- S.J. Thomson, **M.M.P. Couchman**, and J.W.M. Bush. Collective vibrations of confined levitating droplets. *Under review at PRL. arXiv:2001.09165.*
- C.A. Galeano-Rios, **M.M.P. Couchman**, P. Caldairou, and J.W.M. Bush. Ratcheting droplet pairs. *Chaos* (2018)
- S.E. Turton, **M.M.P. Couchman**, and J.W.M. Bush. A review of the theoretical modeling of walking droplets: toward a generalized pilot-wave framework. *Chaos* (2018)

Model of Moláček and Bush (2013)

- drop's vertical dynamics modeled using linear spring

$$m\ddot{Z} + H\left(-Z\right)\left(\Lambda_1 \dot{Z} + \Lambda_2 Z\right) = -mg^*$$

Heaviside function
= 0: free-flight
= 1: contact with bath

Drop's vertical position relative to bath

Effective gravity in vibrating frame

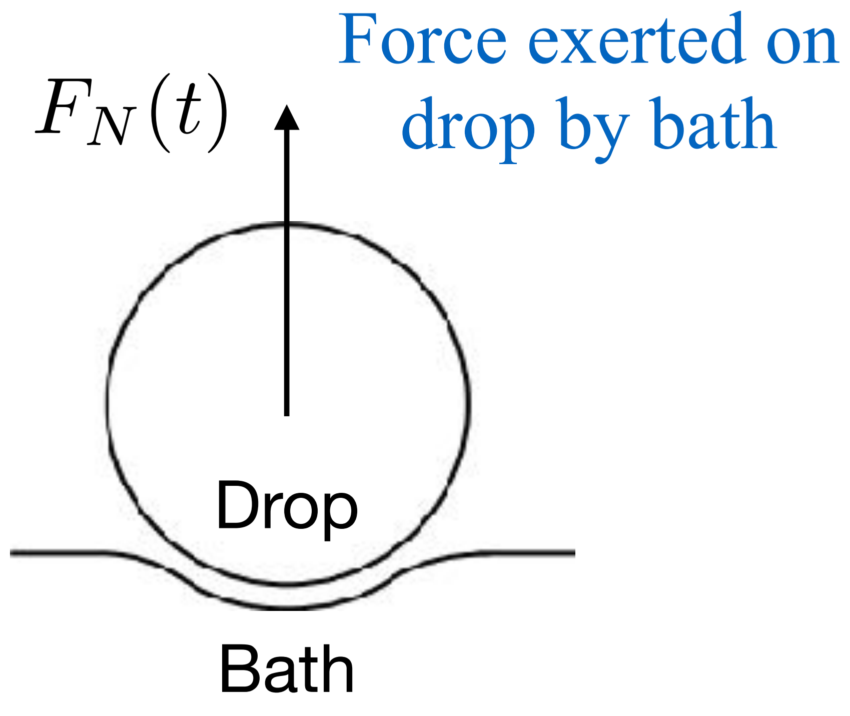

- wavefield generated at previous impacts

$$\mathcal{H}\left(\boldsymbol{x}, t\right) = \sum_n A \boxed{S} \frac{J_0\left(k_F\left|\boldsymbol{x} - \boldsymbol{x}_n\right|\right)}{\sqrt{t - t_n}} e^{-T_d(t-t_n)/(1-\gamma/\gamma_F)}$$

Location of n^{th} impact

Decay time depends on proximity to Faraday threshold

$$\mathcal{S} = \frac{\int F_N\left(t'\right)\sin\left(\pi f t'\right)dt'}{\int F_N\left(t'\right)dt'}$$

Phase of bath oscillation at impact determines amplitude of wave generated

- horizontal trajectory equation

$$m\ddot{\boldsymbol{x}}_p + D\dot{\boldsymbol{x}}_p = -F_N\left(t\right)\nabla\mathcal{H}\left(\boldsymbol{x}_p, t\right)$$

Horizontal wave force proportional to gradient of wavefield at impact

Horizontal and vertical motion coupled through contact force $F_N(t)$

Stroboscopic approximation — Oza *et al.* (2013)

- assume bouncing period is T_F (drop resonant with Faraday waves)

- time-average trajectory equation over bouncing period

$$\int_t^{t+T_F} \left[m\ddot{\boldsymbol{x}}_p + D\dot{\boldsymbol{x}}_p\right] dt' = -\int_t^{t+T_F} \left[F_N\left(t'\right)\nabla\mathcal{H}\left(\boldsymbol{x}_p, t'\right)\right] dt'$$

$$\Downarrow$$

$$m\ddot{\boldsymbol{x}}_p + D\dot{\boldsymbol{x}}_p = -mg\boxed{\mathcal{C}\nabla h\left(\boldsymbol{x}_p, t\right)}$$

Average wave gradient during impact

$$\boxed{C = \frac{\int F_N\left(t'\right)\cos\left(\pi f t'\right) dt'}{\int F_N\left(t'\right) dt'}}$$

Phase of wave oscillation at impact determines horizontal wave force

$$\boxed{h = \frac{\mathcal{H}}{\cos\left(\pi f t\right)}}$$

Wavefield strobed at bouncing frequency

- drop treated as continuous source of waves

$$h\left(\boldsymbol{x}, t\right) = A\int_{-\infty}^{t} \mathcal{S} J_0\left(k_F\left|\boldsymbol{x} - \boldsymbol{x}\left(s\right)\right|\right) e^{-T_d(t-s)/(1-\gamma/\gamma_F)} ds$$

- vertical dynamics assumed to be constant: $\mathcal{S}$ and $\mathcal{C}$ replaced by unspecified parameter $\sin\Phi$

Impact phase parameters

- coupling between horizontal and vertical motion captured by two phase parameters:
  - $\mathcal{S} = \dfrac{\int F_N\left(t'\right)\sin\left(\pi f t'\right)dt'}{\int F_N\left(t'\right)dt'}$ **Phase of bath oscillation** at which droplet impacts $\longrightarrow$ Determines **wave amplitude**
  - $C = \dfrac{\int F_N\left(t'\right)\cos\left(\pi f t'\right)dt'}{\int F_N\left(t'\right)dt'}$ **Phase of wave oscillation** at which droplet impacts $\longrightarrow$ Determines **wave force**

- $\mathcal{S}$ and $\mathcal{C}$ expected to depend on drop radius R, vibrational acceleration γ, local wave amplitude $h_p = h\left(\boldsymbol{x}_p, t\right)$

- **Goal**: develop functional forms $\mathcal{S} = \mathcal{S}\left(\gamma, h_p, R\right)$ and $\mathcal{C} = \mathcal{C}\left(\gamma, h_p, R\right)$
  - use in stroboscopic model to obtain trajectory equation that captures weak variations in vertical dynamics

Experimental set-up

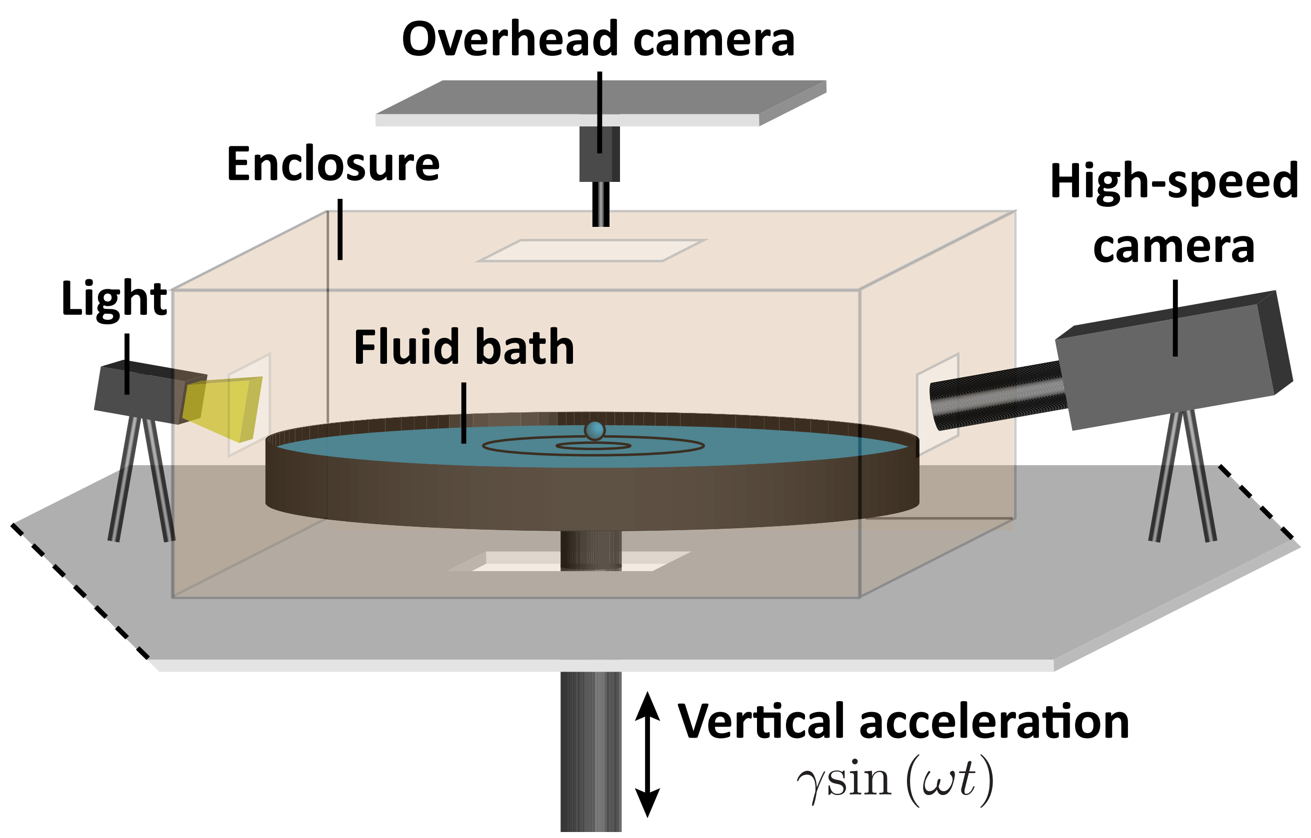

100x slower than reality

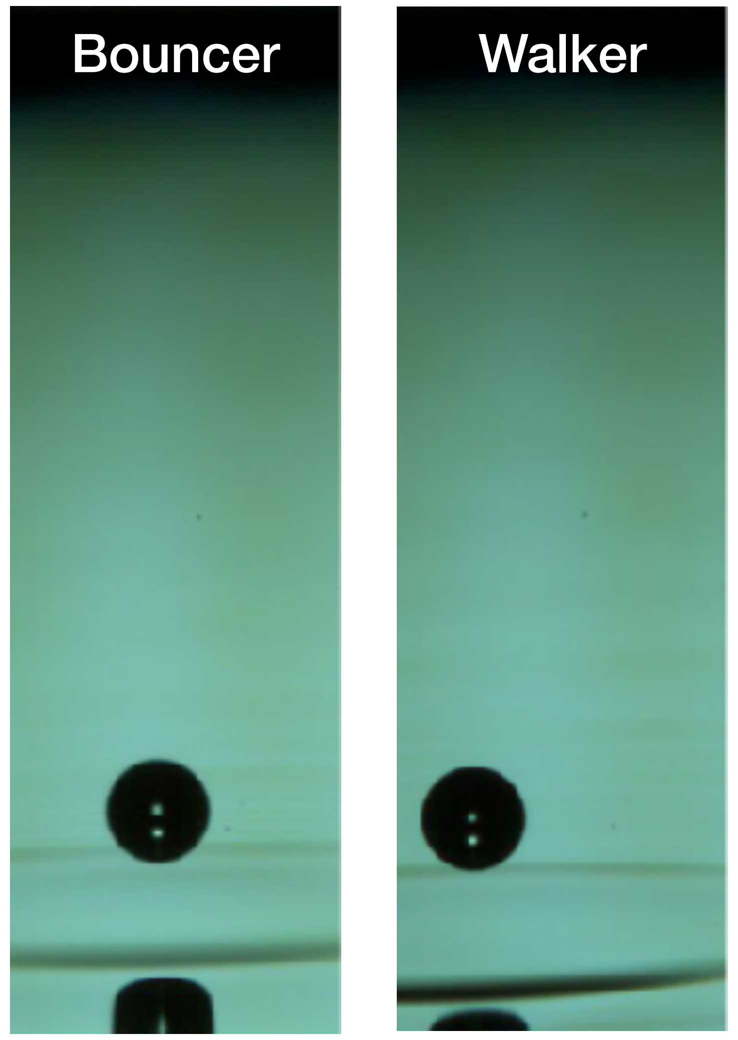

Dependence of bouncing mode on dimensionless drop size and vibrational acceleration

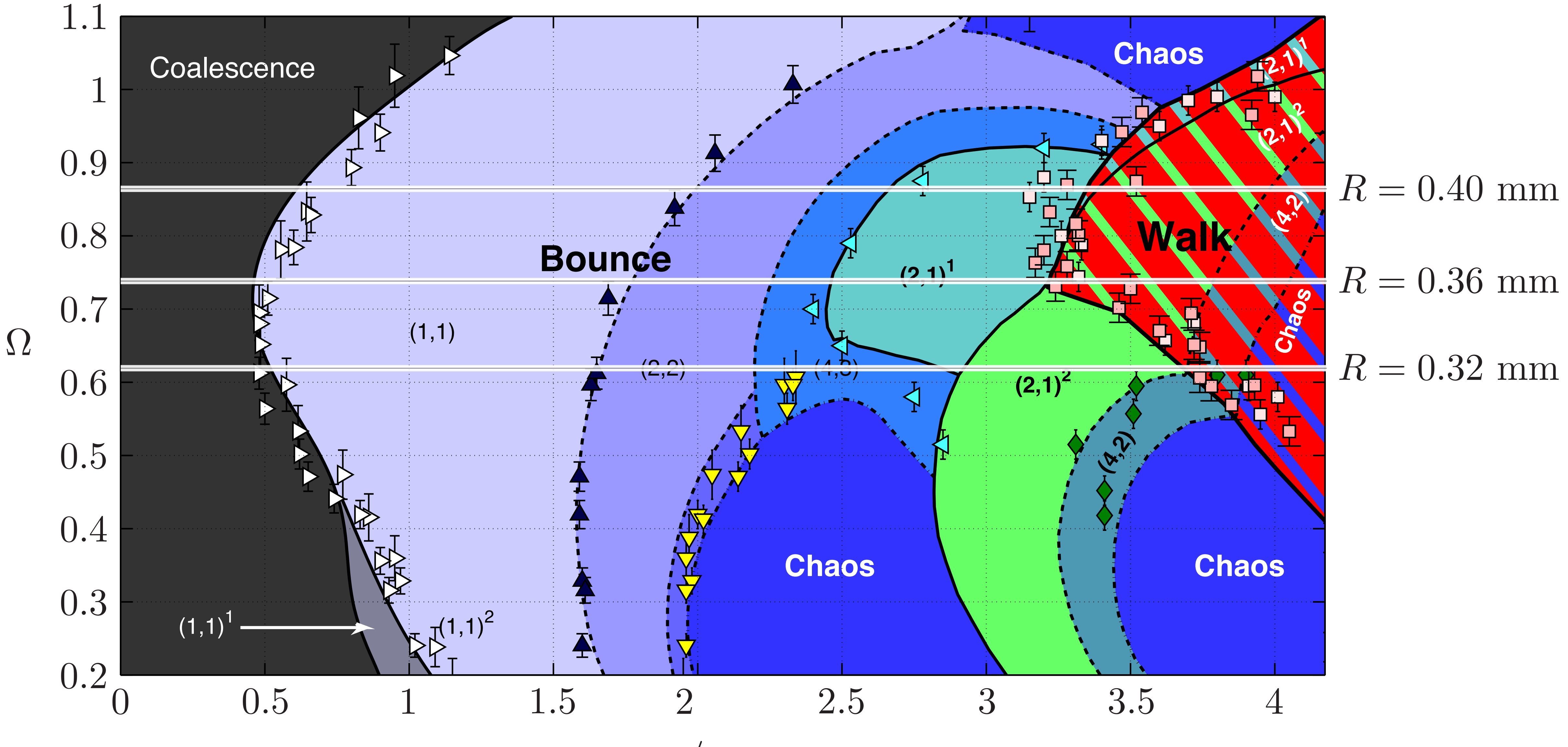

Moláček and Bush 2013; Wind-Willassen *et al.* 2013

- use high-speed imaging to directly measure drop's vertical motion
- consider three drop sizes that span resonant $(2,1)$ bouncing mode

- Bouncing mode notation: $(i,j)^k$
  - Drop's bouncing period i times that of bath vibration, $T_F/2$, impacts bath j times during this period
  - $k = \{1,2\}$: small- or large-amplitude bouncing for same mode

Experimental measurements of phase parameters

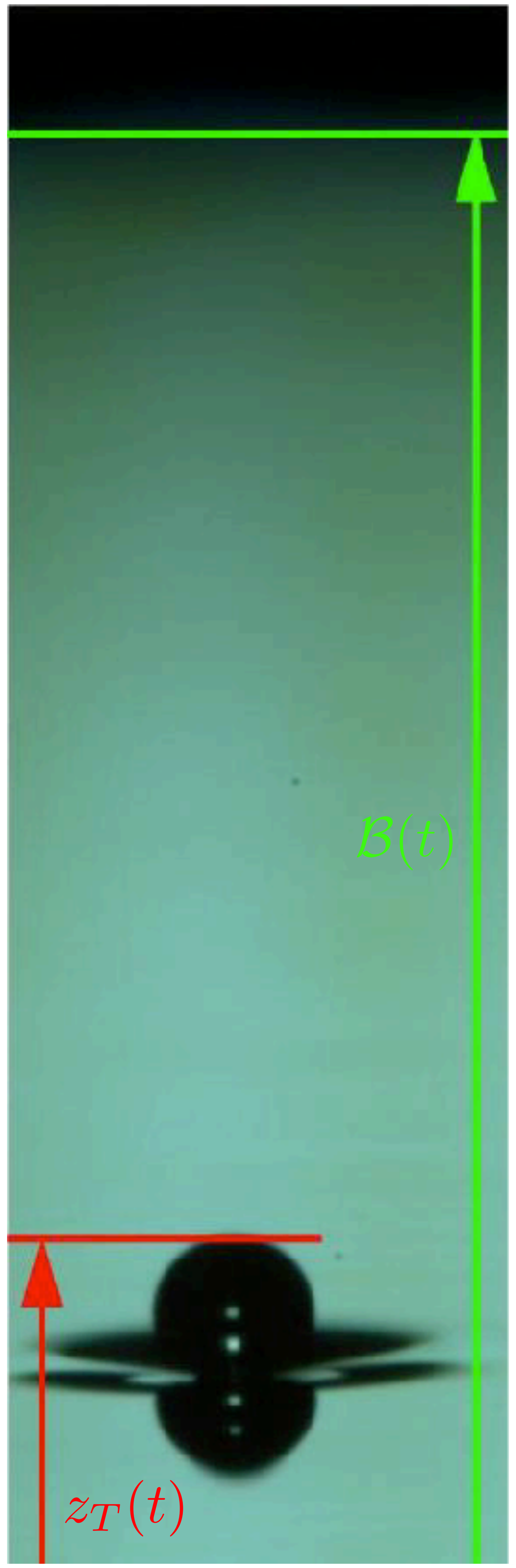

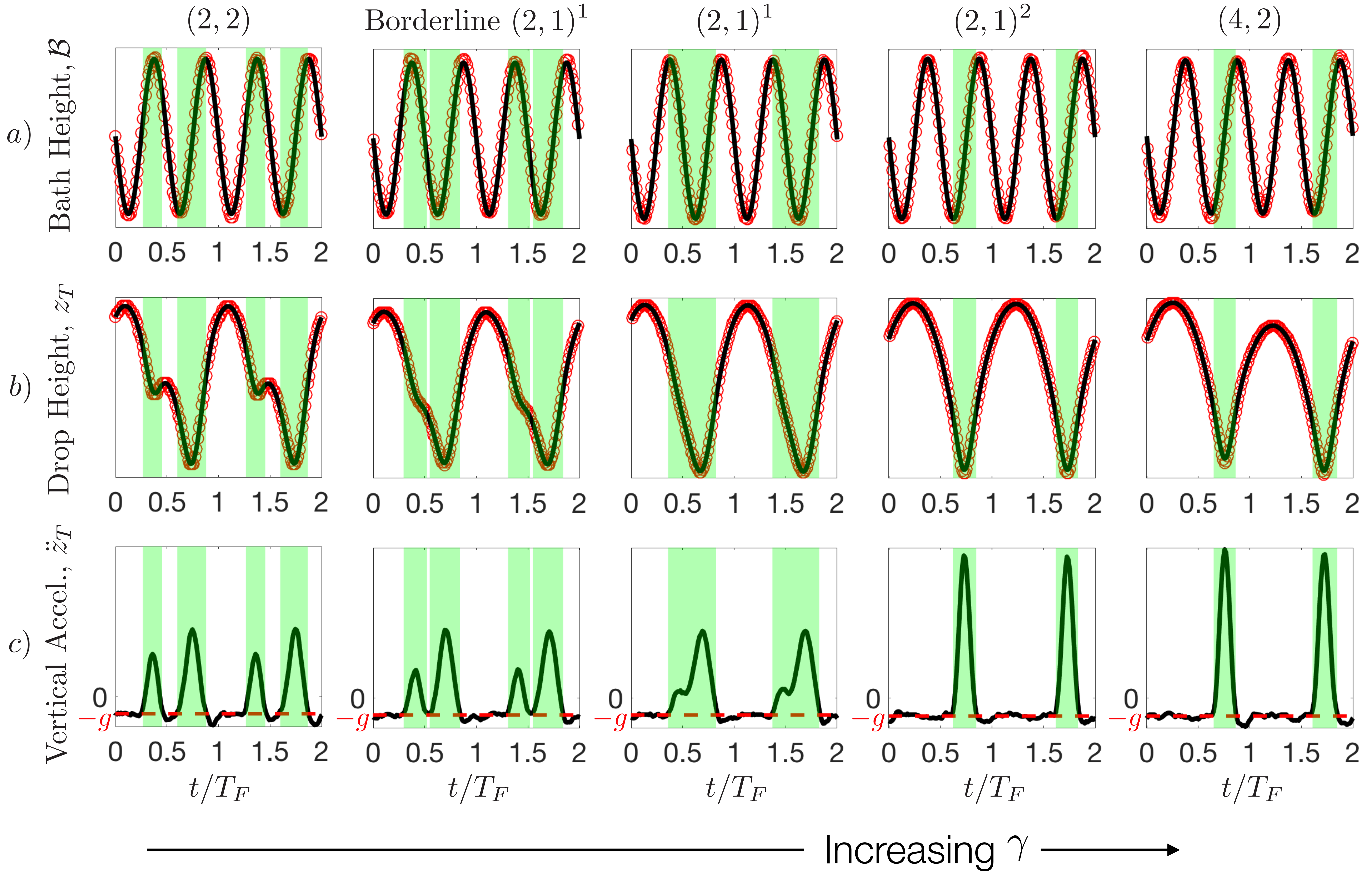

$$\mathcal{S} = \frac{\int F_N(t') \sin(\pi f t')\, dt'}{\int F_N(t')\, dt'}$$

$$\mathcal{C} = \frac{\int F_N(t') \cos(\pi f t')\, dt'}{\int F_N(t')\, dt'}$$

- deduce contact force $F_N(t)$ from $\ddot{z}_T(t)$, obtain phase parameters $\mathcal{S}$ and $\mathcal{C}$
- first measurements of contact force for bouncers and walkers

Phase parameters for single droplets

- impact phase varies significantly with drop radius and vibrational acceleration
- different behaviors for drops in low-amplitude $(2,1)^1$ and high-amplitude $(2,1)^2$ bouncing modes

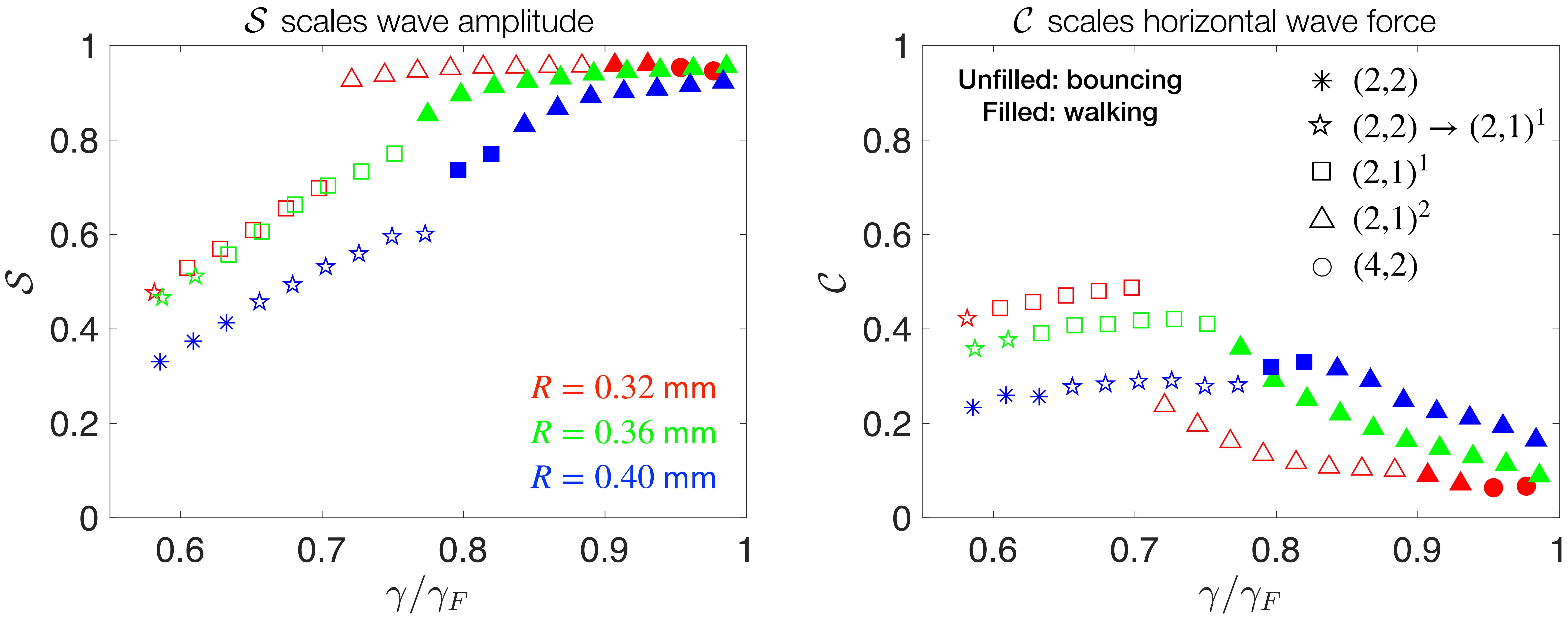

Theoretical model for phase parameters

- liquid surface beneath drop:

$$\mathcal{A}(\tau) = \underbrace{-\frac{\gamma}{R\omega^2}\sin(\Omega\tau)}_{\substack{\text{Harmonic}\\ \text{bath oscillation}}} + \underbrace{\frac{h_p}{R}\cos(\Omega\tau/2)}_{\substack{\text{Subharmonic}\\ \text{wave oscillation}}}$$

- consider reference frame where liquid beneath drop is stationary: $\mathcal{Z} = z - \mathcal{A}$

- seek exact $(2,1)$ solutions to linear spring model of Moláček and Bush (2013) as function of R, γ, $h_p = h(\boldsymbol{x}_p, t)$

$$\ddot{\mathcal{Z}} + H(-\mathcal{Z})\left(\Lambda_1\dot{\mathcal{Z}} + \Lambda_2\mathcal{Z}\right) = \underbrace{-Bo\left(1 + \frac{\gamma}{g}\sin(\Omega\tau) - \frac{h_p R\omega^2}{4g}\cos\left(\frac{\Omega\tau}{2}\right)\right)}_{\text{Effective gravity in stationary frame}}$$

- deduce theoretical phase functions:

$$\mathcal{S} = \mathcal{S}(\gamma, h_p, R)\,,\;\; \mathcal{C} = \mathcal{C}(\gamma, h_p, R)$$

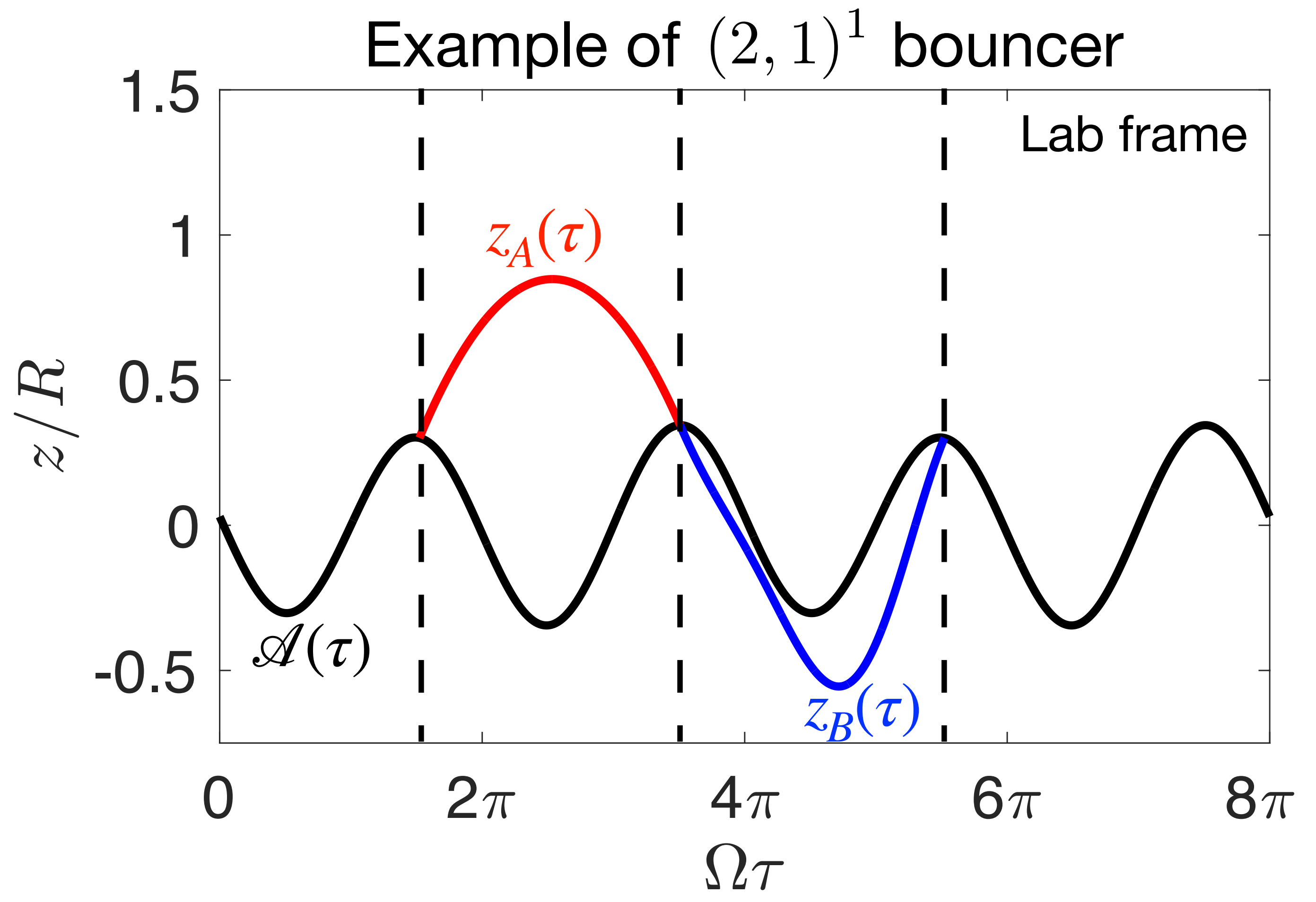

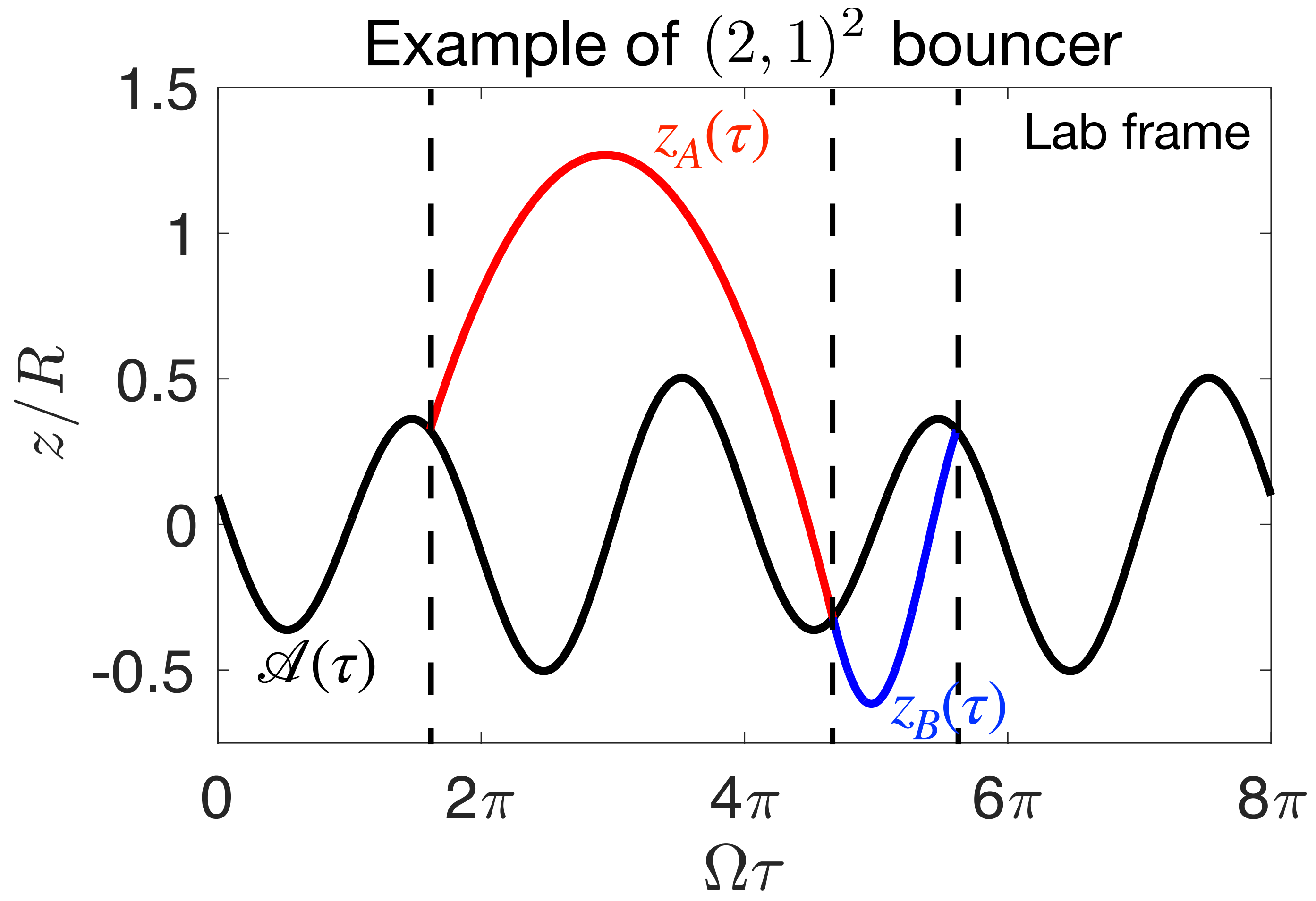

Theoretical model for phase parameters

- for given R, sweep through γ and h_p to determine $\mathcal{S}$ and $\mathcal{C}$ in $(2,1)^1$ and $(2,1)^2$ modes

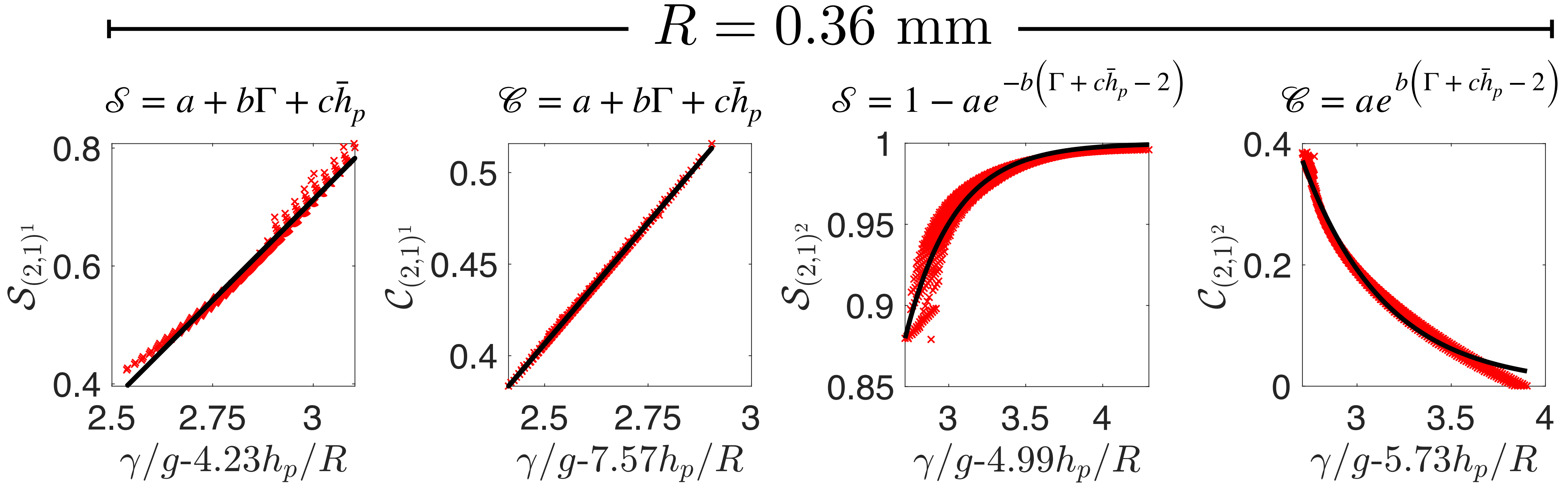

Coefficients depend linearly on drop size

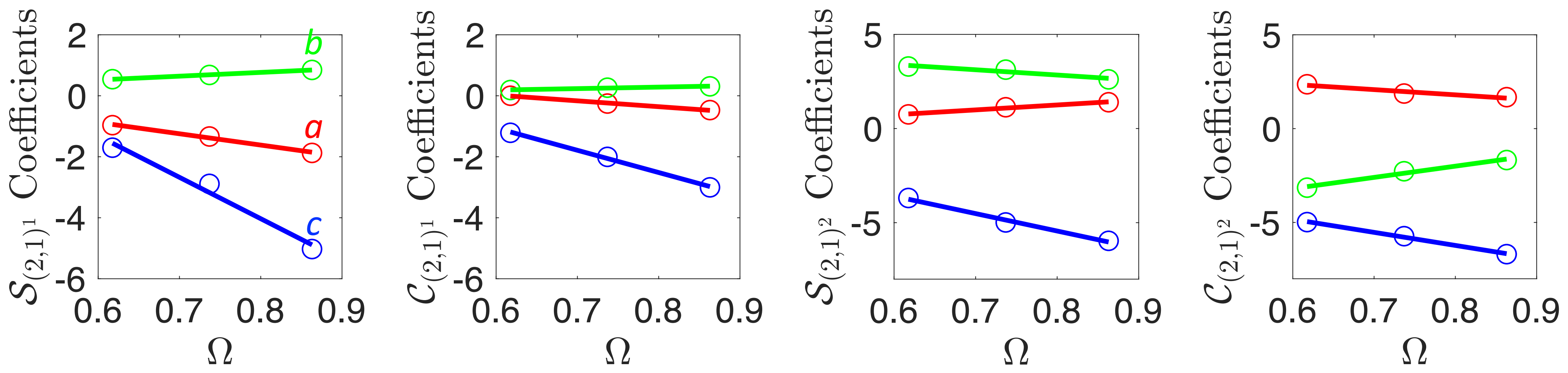

- yields theoretical phase functions that can be used in stroboscopic trajectory equation

Phase Param.	Functional Form	Parameter Values		
$\mathcal{S}_{(2,1)^1}$	$a + b\Gamma + c\bar{h}_p$	$a = -3.71\Omega + 1.35$,	$b = 1.24\Omega - 0.224$,	$c = -13.6\Omega + 6.83$
$\mathcal{C}_{(2,1)^1}$	$a + b\Gamma + c\bar{h}_p$	$a = -1.92\Omega + 1.17$,	$b = 0.490\Omega - 0.108$,	$c = -7.29\Omega + 3.32$
$\mathcal{S}_{(2,1)^2}$	$1 - ae^{-b(\Gamma + c\bar{h}_p - 2)}$	$a = 1.79\Omega$,	$b = -5.60\Omega + 7.65$,	$c = -8.00\Omega + 0.168$
$\mathcal{C}_{(2,1)^2}$	$ae^{-b(\Gamma + c\bar{h}_p - 2)}$	$a = -3.55\Omega + 4.60$,	$b = -6.06\Omega + 6.84$,	$c = -8.57\Omega + 0.453$

Variable-impact-phase trajectory equation

- trajectory equation now accounts for modulations in vertical dynamics

$$\kappa \ddot{\boldsymbol{x}}_p + \dot{\boldsymbol{x}}_p = -\beta \overbrace{\mathcal{C}\left(\gamma, h_p, R\right)}^{\text{scales horizontal wave force}} \nabla h\left(\boldsymbol{x}_p, t\right)$$

$$h\left(\boldsymbol{x}, t\right) = A \int_{-\infty}^{t} \underbrace{\mathcal{S}\left(\gamma, h_p R\right)}_{\text{scales wave amplitude}} J_0\left(\left|\boldsymbol{x} - \boldsymbol{x}_p\left(s\right)\right|\right) e^{-(t-s)} ds$$

- valid for drops in resonant $(2, 1)$ bouncing mode
    - regime of interest for hydrodynamic quantum analogs

Walking speeds and thresholds

- model captures dependence of impact phase on drop size and vibrational acceleration.
- more accurately predicts walking thresholds and speeds, with no fitting parameters.

Equations governing single droplet walking at speed u

$$h_p = \frac{A\mathcal{S}(\gamma, h_p, R)\, T_D}{R\,(1-\gamma/\gamma_F)\sqrt{1+u^2}}$$

$$u = \sqrt{\phi - \frac{1}{2}\left(1+\sqrt{1+4\phi}\right)}$$

$$\phi = \frac{A\beta T_D \mathcal{S}(\gamma, h_p, R)\,\mathcal{C}(\gamma, h_p, R)}{R\,(1-\gamma/\gamma_F)}$$

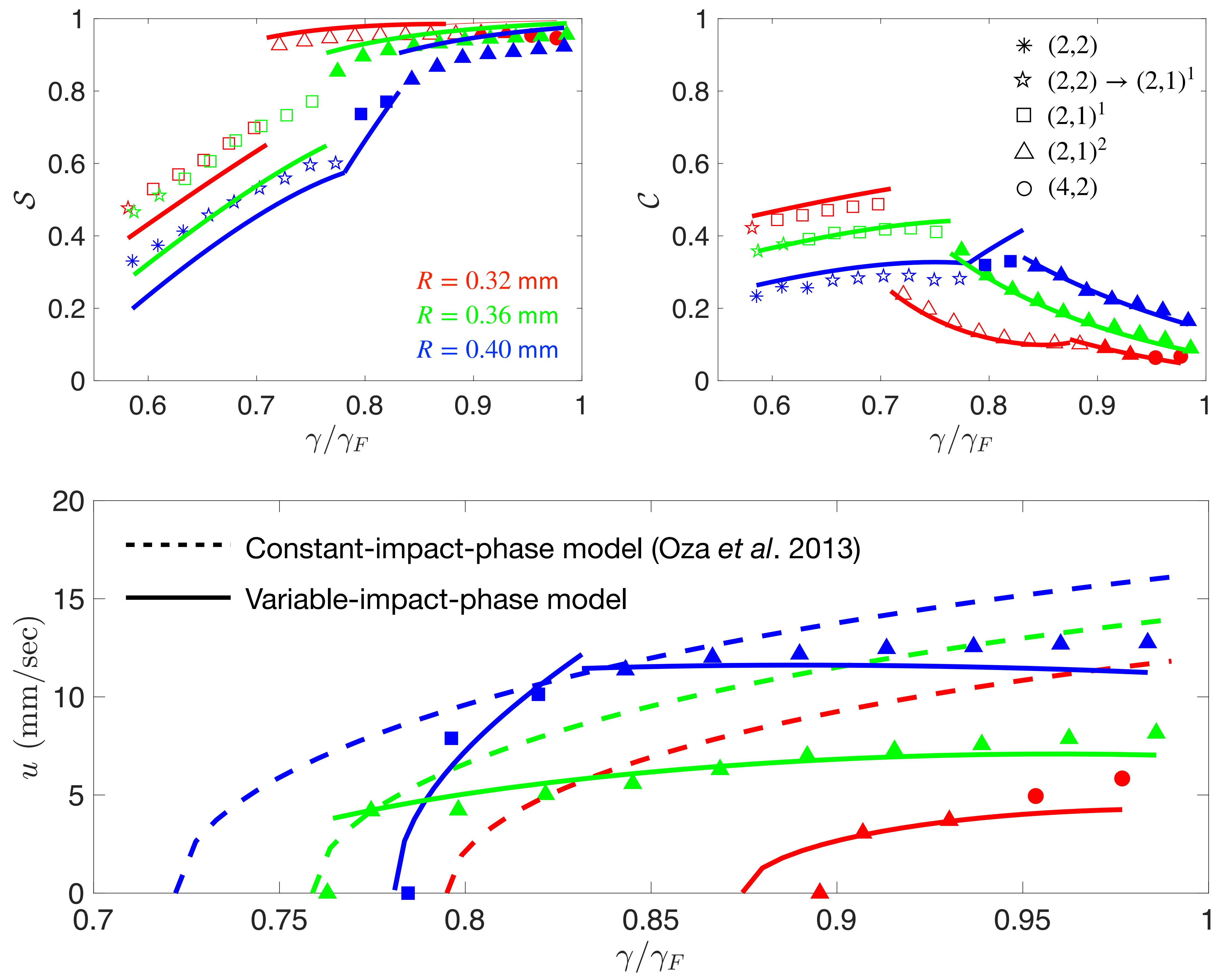

The stability of droplet pairs

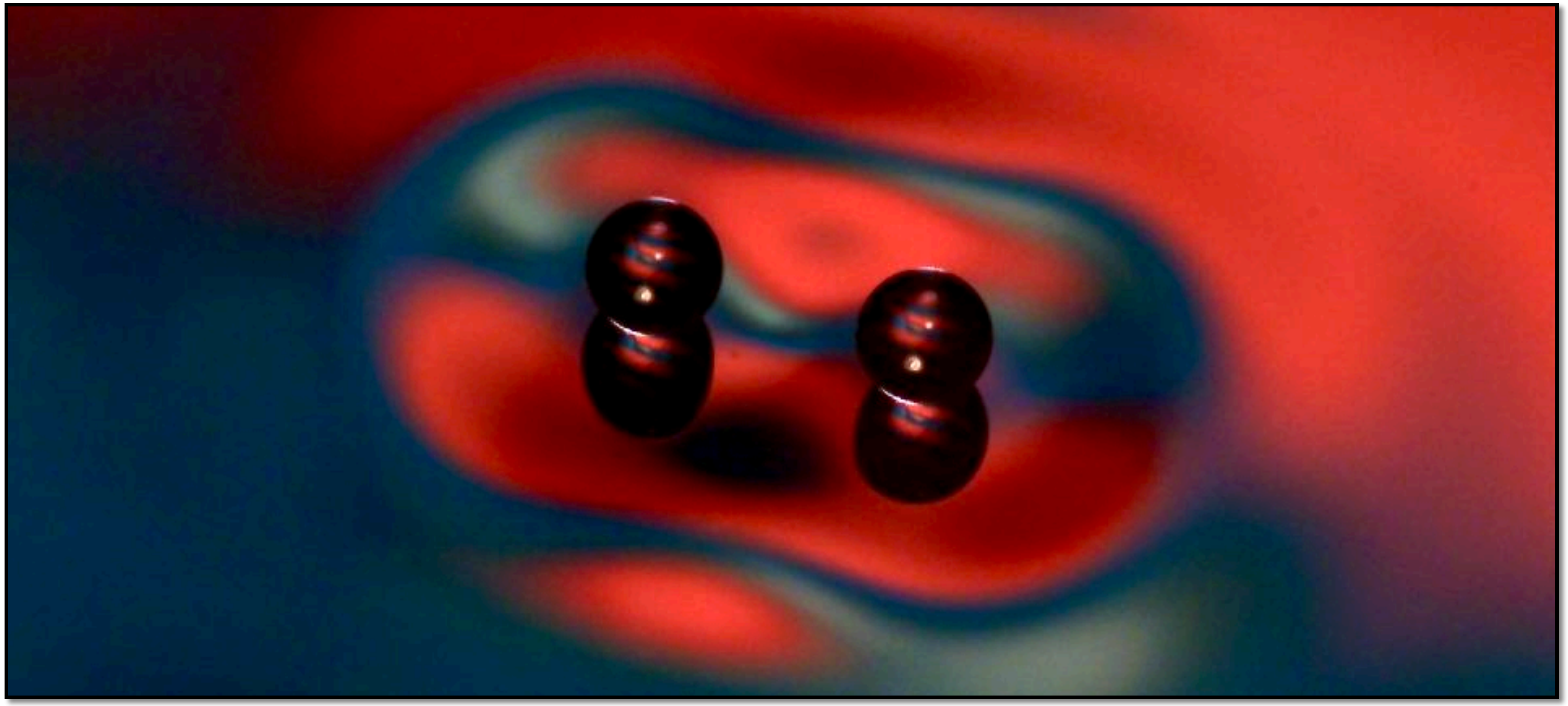

J. Fluid Mech. (2019), vol. 871, pp. 212–243. © Cambridge University Press 2019 212
doi:10.1017/jfm.2019.293

Bouncing phase variations in pilot-wave hydrodynamics and the stability of droplet pairs

Miles M. P. Couchman[1], Sam E. Turton[1] and John W. M. Bush[1,†]

[1]Department of Mathematics, Massachusetts Institute of Technology, Cambridge, MA 02139, USA

- How do stationary bound pairs destabilize as bath's vibrational acceleration γ is increased?
- Instability depends on inter-drop distance d and droplet radius R

Quantized set of bound states

- each drop must bounce in minimum of neighbor's wavefield in order to remain stationary
- as vibrational acceleration γ increases, additional quantized states emerge due to increased spatial extent of wavefield

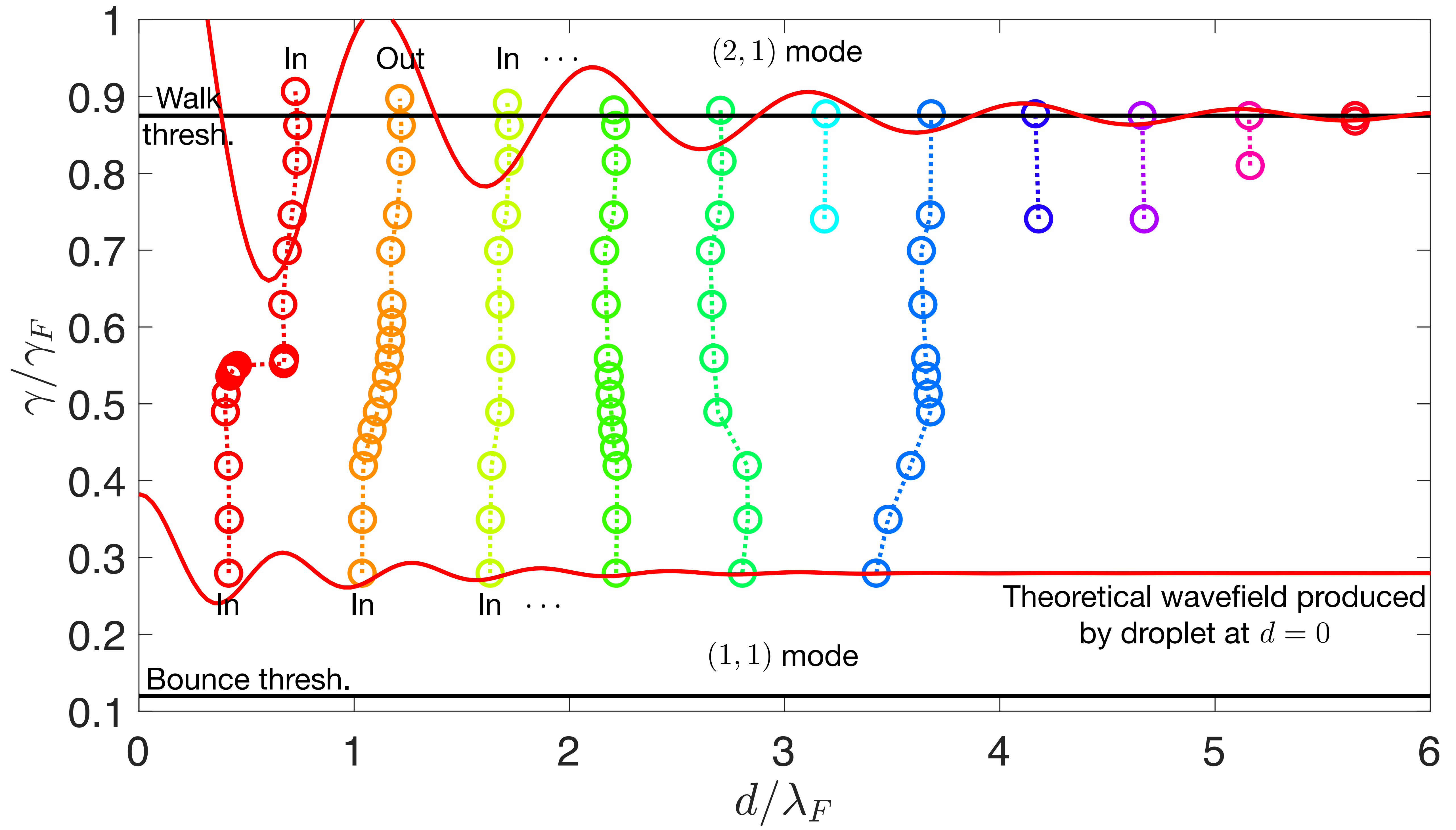

$(2, 1)$ bouncers (40 Hz)

- In- or out-of-phase
- $\lambda_F = 4.75$ mm

$(1, 1)$ bouncers (80 Hz)

- Always in-phase
- $\lambda_F = 2.86$ mm

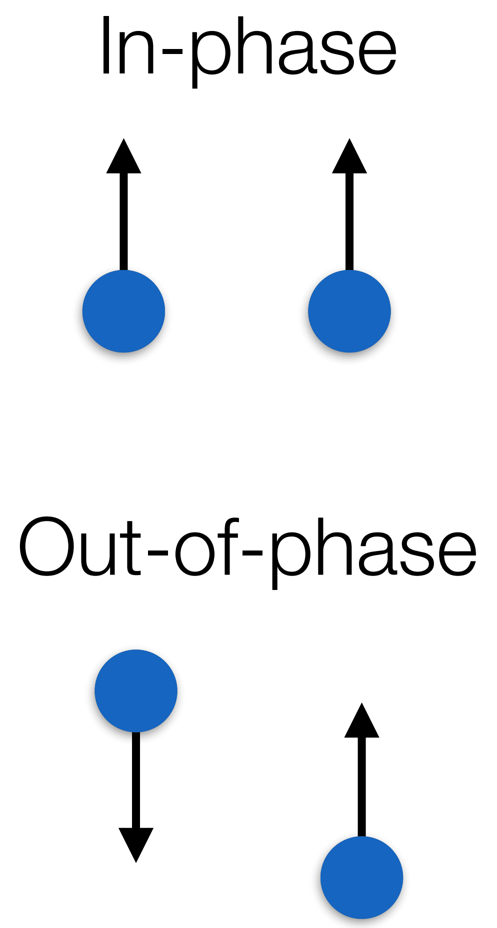

Type and threshold of instability

- different instability for pairs in low-amplitude $(2,1)^1$ and high-amplitude $(2,1)^2$ bouncing mode

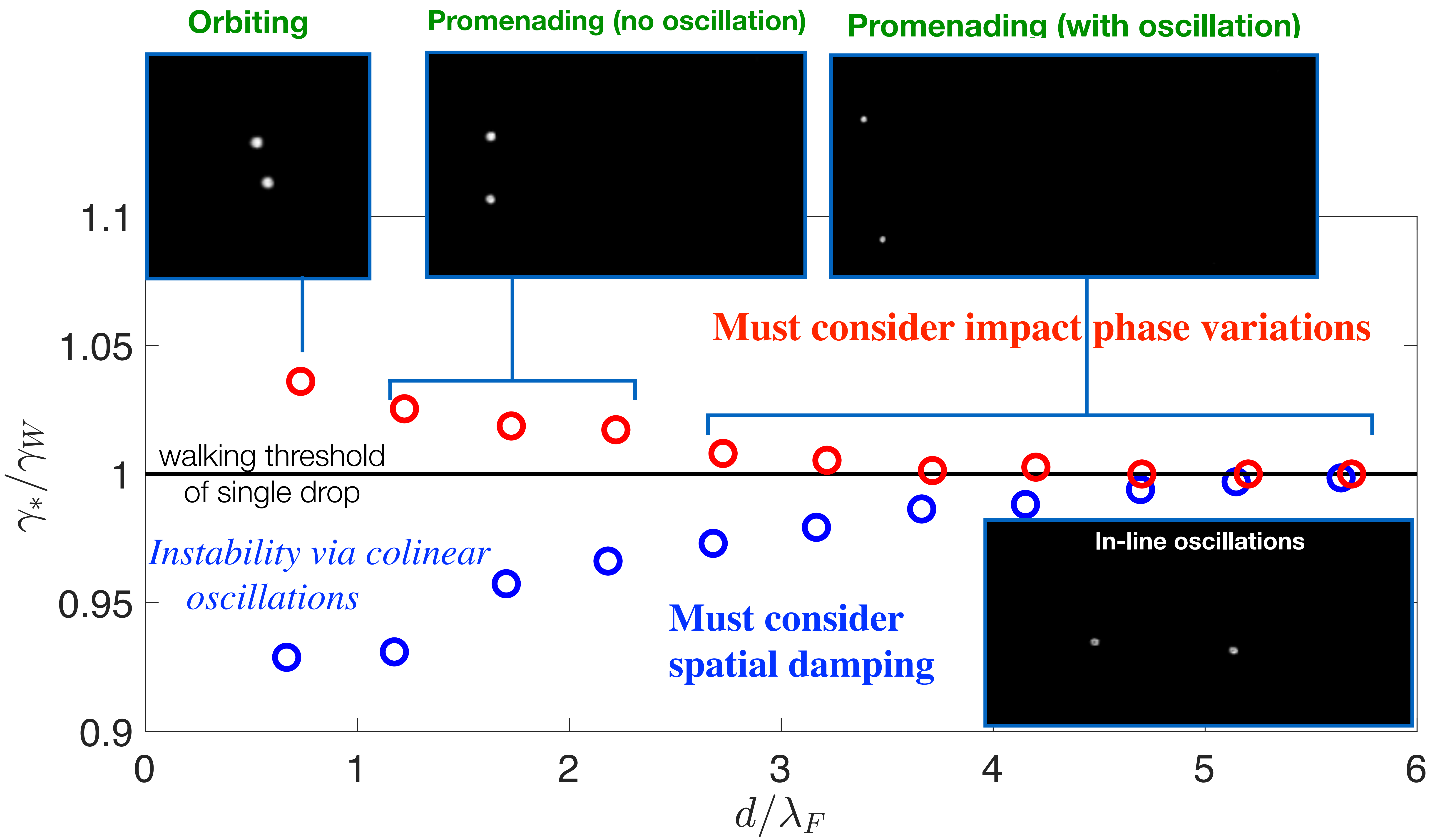

$(2,1)^2,\ R = 0.32$ mm

- Stabilization
- Transverse instability

$(2,1)^1,\ R = 0.40$ mm

- Destabilization
- Radial instability

Strobed equations of motion (Oza *et al.*, 2013)

$$\kappa\ddot{\vec{x}}_1 + \dot{\vec{x}}_1 = F_{11} + \sigma F_{21}$$

$$\kappa\ddot{\vec{x}}_2 + \dot{\vec{x}}_2 = F_{22} + \sigma F_{12}$$

F_{ij}: wave-force produced by j^{th} drop acting on i^{th} drop

$\sigma = \pm 1$ if drops are in (+) or out (-) of phase

$$F_{ij} = \beta \int_{-\infty}^{t} J_1\left(\left|\vec{x}_j(t) - \vec{x}_i(s)\right|\right) \frac{\vec{x}_j(t) - \vec{x}_i(s)}{\left|\vec{x}_j(t) - \vec{x}_i(s)\right|} e^{-(t-s)} ds$$

Re-write equations in center-of-mass frame:

$$(\vec{x}_1, \vec{x}_2) \rightarrow \left(\vec{X}, \vec{r}\right)$$

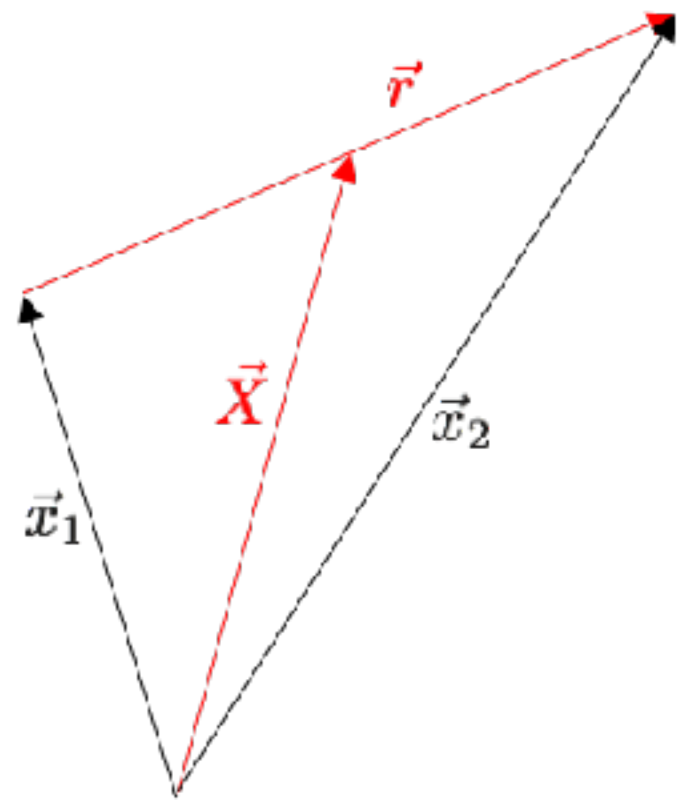

Pure oscillations governed by:

$$\ddot{r} = \frac{\sigma\beta}{\kappa}\left[\underbrace{\left(\frac{\beta-2}{2\sigma\beta} - \frac{J_1(r)}{r} + J_2(r)\right)\dot{r}}_{\text{Non-linear damping}} + \underbrace{2J_1(r)}_{\text{Non-linear spring force}}\right]$$

`Large' bouncing pairs: apply strobe model w spatial damping

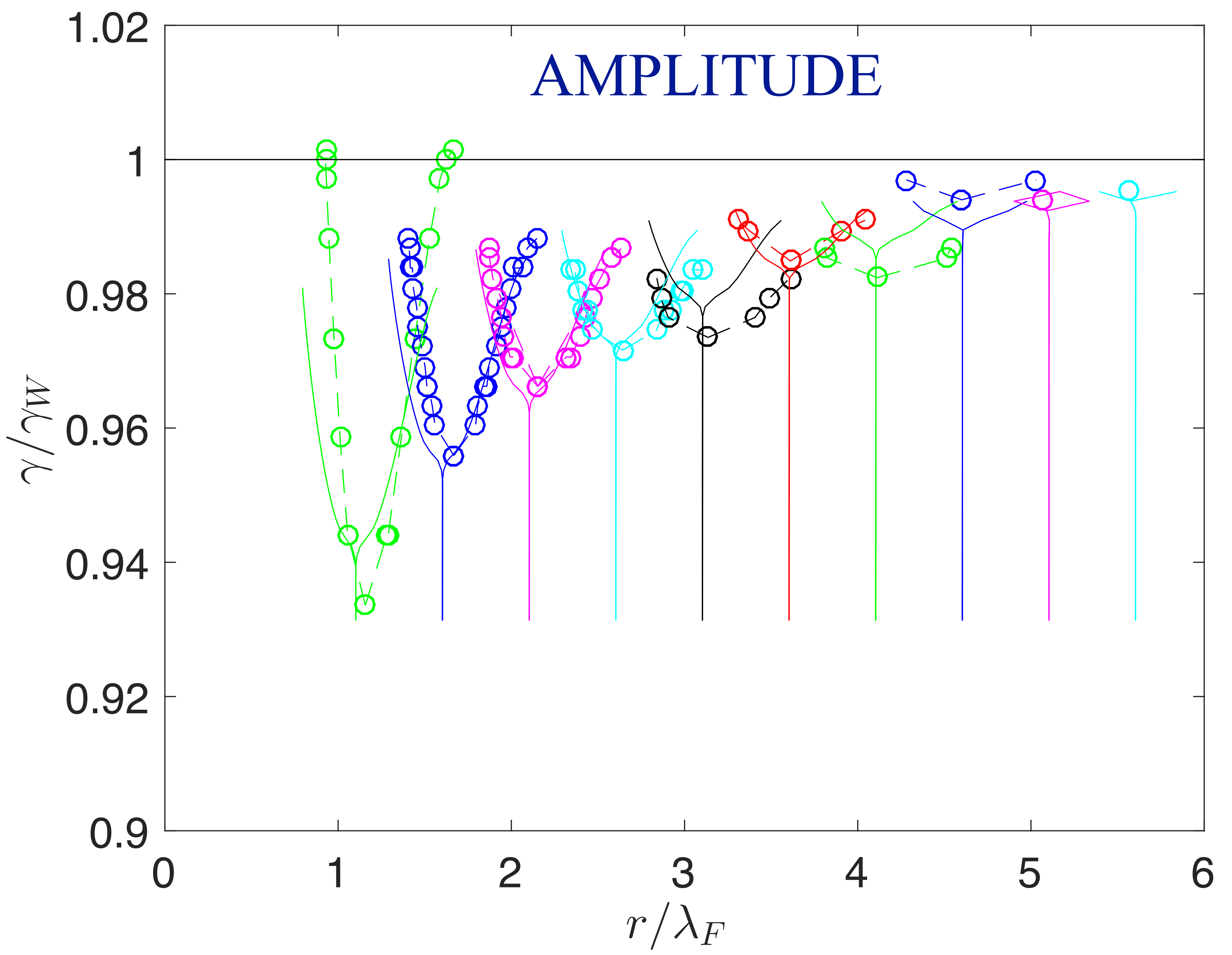

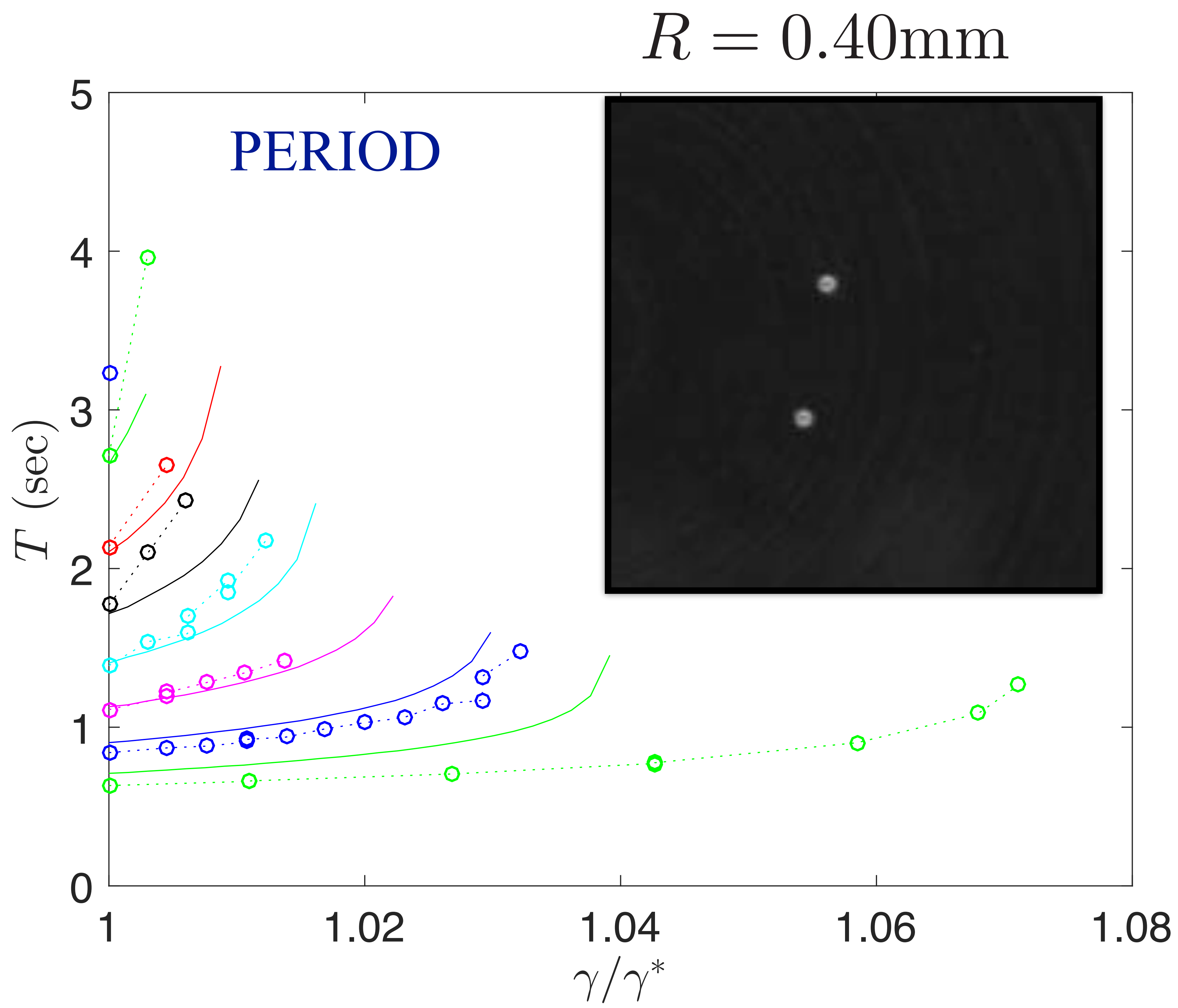

- in center-of-mass frame, inter-drop distance **r** evolves according to

$$\kappa\ddot{r} + \dot{r} = 2\beta \int_{-\infty}^{t} \left\{ \left[J_1(r_-) + \frac{2\bar{\alpha}r_-}{t-s} J_0(r_-) \right] e^{-\frac{\bar{\alpha}r_-^2}{t-s}} + \sigma \left[J_1(r_+) + \frac{2\bar{\alpha}r_+}{t-s} J_0(r_+) \right] e^{-\frac{\bar{\alpha}r_+^2}{t-s}} \right\} e^{-(t-s)} ds$$

where $r_- \equiv \dfrac{r(t) - r(s)}{2}$, $r_+ \equiv \dfrac{r(t) + r(s)}{2}$, $\sigma = \pm 1$ when drops in (+) or out-of (-) phase

- indicates importance of spatial damping on stability characteristics

`Small' bouncing pairs: also need to consider phase variations

- consideration of vertical dynamics yields dependence of bouncing phase on both memory and local wave amplitude *a*
- bouncing phase thus depends on separation distance of bouncing pairs
- the resulting phase variation is important for the smaller drops

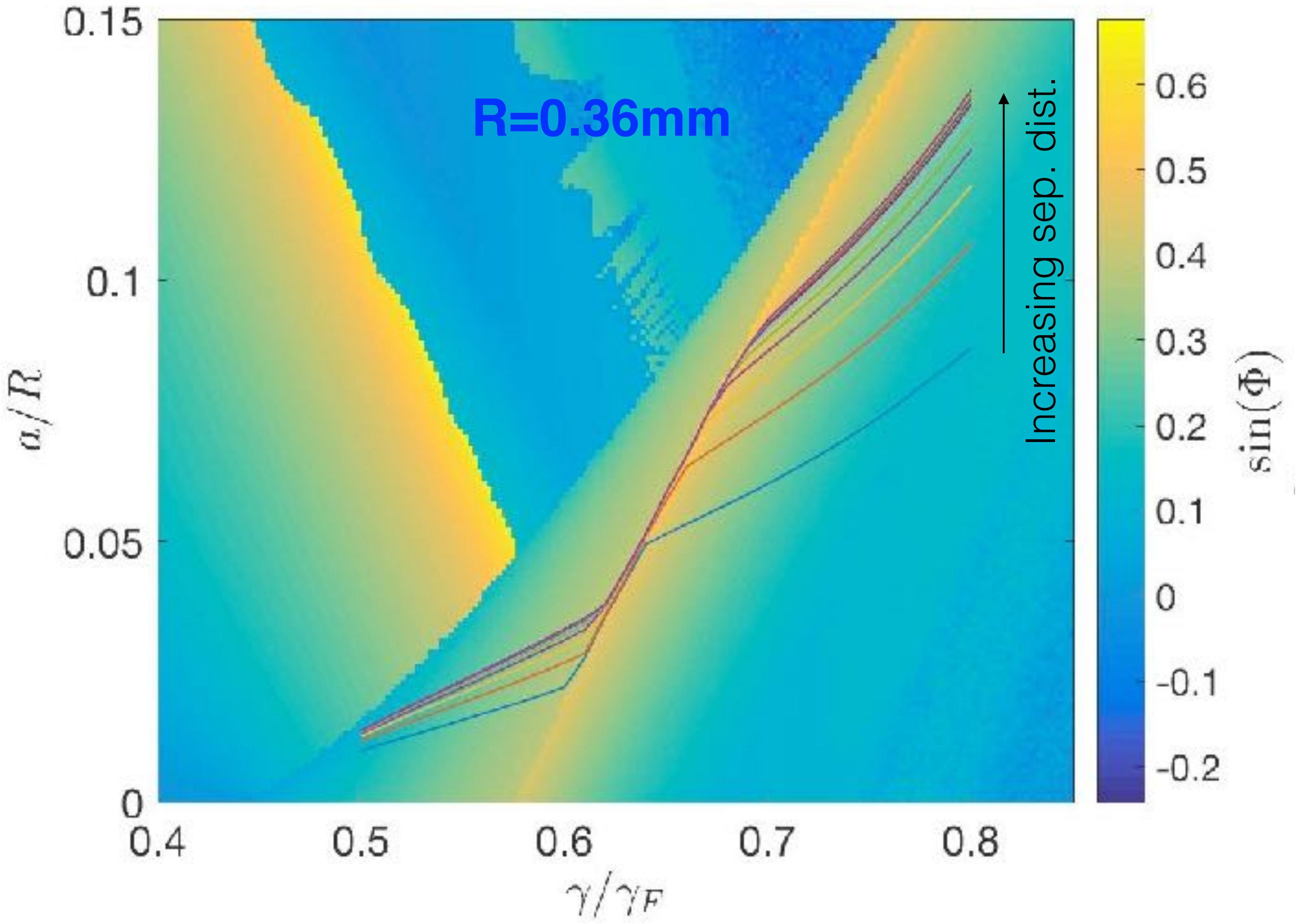

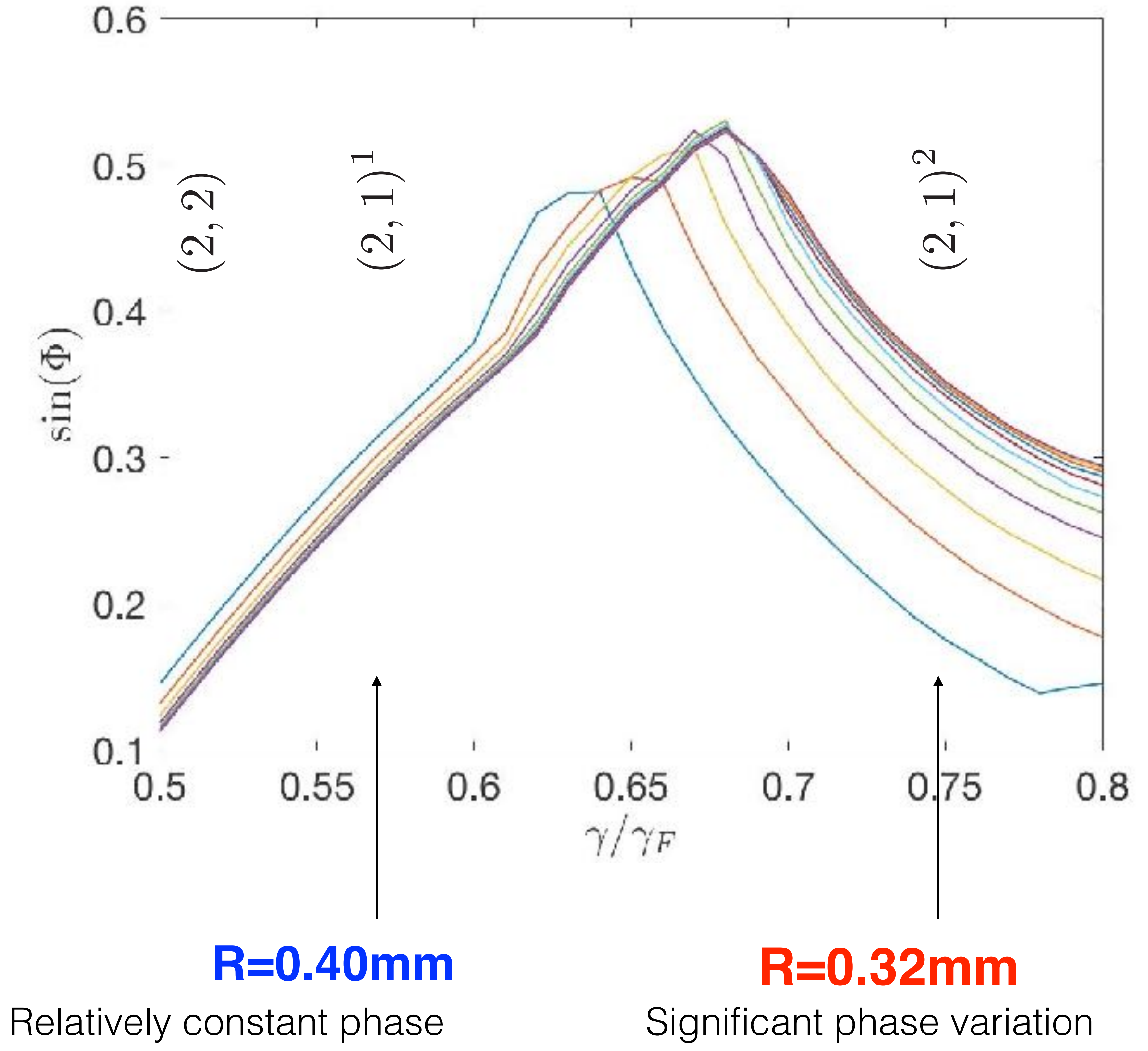

- applies whenever bouncing phase varies: orbits, promenaders, ratchets…

Linear stability analysis

- variable-impact-phase trajectory equation for multiple interacting droplets

$$\kappa\ddot{\boldsymbol{x}}_m + \dot{\boldsymbol{x}}_m = -\beta\sigma_m\mathcal{C}_m\nabla h\left(\boldsymbol{x}_m, t\right)$$

Trajectory equation for m^{th} drop

$$h\left(\boldsymbol{x}, t\right) = A\sum_{n=1}^{N}\sigma_n\int_{-\infty}^{t}\mathcal{S}_n f\left(\left|\boldsymbol{x} - \boldsymbol{x}_n\left(s\right)\right|\right)e^{-(t-s)}ds$$

Wavefield strobed at bouncing period

$$f\left(r\right) = J_0\left(r\right)\left[1 + \left(\xi K_1\left(\xi r\right)r - 1\right)e^{-\left(1/r^2\right)}\right]$$

Wave kernel with spatial-damping

(see: Damiano *et al*. 2016; Tadrist *et al*. 2018; Turton *et al*. 2018; Couchman *et al*. 2019)

- stationary bouncing state: inter-drop distance must satisfy $f'\left(d_0\right) = 0$

- consider arbitrary perturbations:

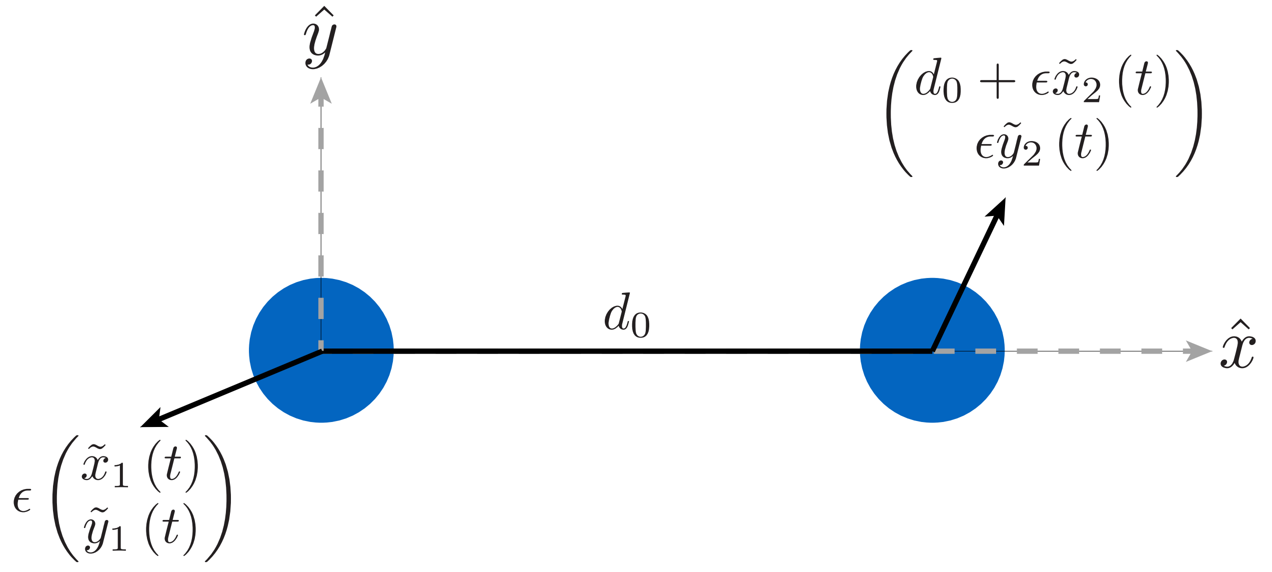

Linear stability analysis

- obtain block-diagonal linear system that correctly predicts the three observed types of instability

In-line walking

In-line oscillations

$$
\frac{d}{dt}\begin{pmatrix} \boxed{\begin{matrix} x_1+x_2 \\ u_1+u_2 \\ X_1+X_2 \end{matrix}} \\ \boxed{\begin{matrix} x_1-x_2 \\ u_1-u_2 \\ X_1-X_2 \end{matrix}} \\ \boxed{\begin{matrix} y_1 \\ v_1 \\ Y_1 \end{matrix}} \\ \boxed{\begin{matrix} y_2 \\ v_2 \\ Y_2 \end{matrix}} \end{pmatrix} = \begin{pmatrix} \boxed{\begin{pmatrix} 0 & 1 & 0 \\ A-B & -\frac{1}{\kappa} & B-A \\ 1 & 0 & -1 \end{pmatrix}} & 0 & 0 & 0 \\ 0 & \boxed{\begin{pmatrix} 0 & 1 & 0 \\ A-B & -\frac{1}{\kappa} & -A-B \\ 1 & 0 & -1 \end{pmatrix}} & 0 & 0 \\ 0 & 0 & \boxed{\begin{pmatrix} 0 & 1 & 0 \\ A & -\frac{1}{\kappa} & -A \\ 1 & 0 & -1 \end{pmatrix}} & 0 \\ 0 & 0 & 0 & \boxed{\begin{pmatrix} 0 & 1 & 0 \\ A & -\frac{1}{\kappa} & -A \\ 1 & 0 & -1 \end{pmatrix}} \end{pmatrix} \begin{pmatrix} \boxed{\begin{matrix} x_1+x_2 \\ u_1+u_2 \\ X_1+X_2 \end{matrix}} \\ \boxed{\begin{matrix} x_1-x_2 \\ u_1-u_2 \\ X_1-X_2 \end{matrix}} \\ \boxed{\begin{matrix} y_1 \\ v_1 \\ Y_1 \end{matrix}} \\ \boxed{\begin{matrix} y_2 \\ v_2 \\ Y_2 \end{matrix}} \end{pmatrix}
$$

Transverse instabilities

$$X_i(t) = \int_{-\infty}^{t} x_i(s)\, e^{-(t-s)} ds$$

$$A = \frac{\beta}{\kappa} \boxed{\mathcal{C}_0 \mathcal{S}_0} f''(0)$$

$$B = \frac{\beta}{\kappa} \boxed{\mathcal{C}_0 \mathcal{S}_0} f''(d_0)$$

- vertical dynamics influence stability through $\mathcal{S}_0$ and $\mathcal{C}_0$ (values of phase parameters in base state)

Influence of vertical dynamics on stability

- only variable-impact-phase model is able to capture observed instabilities

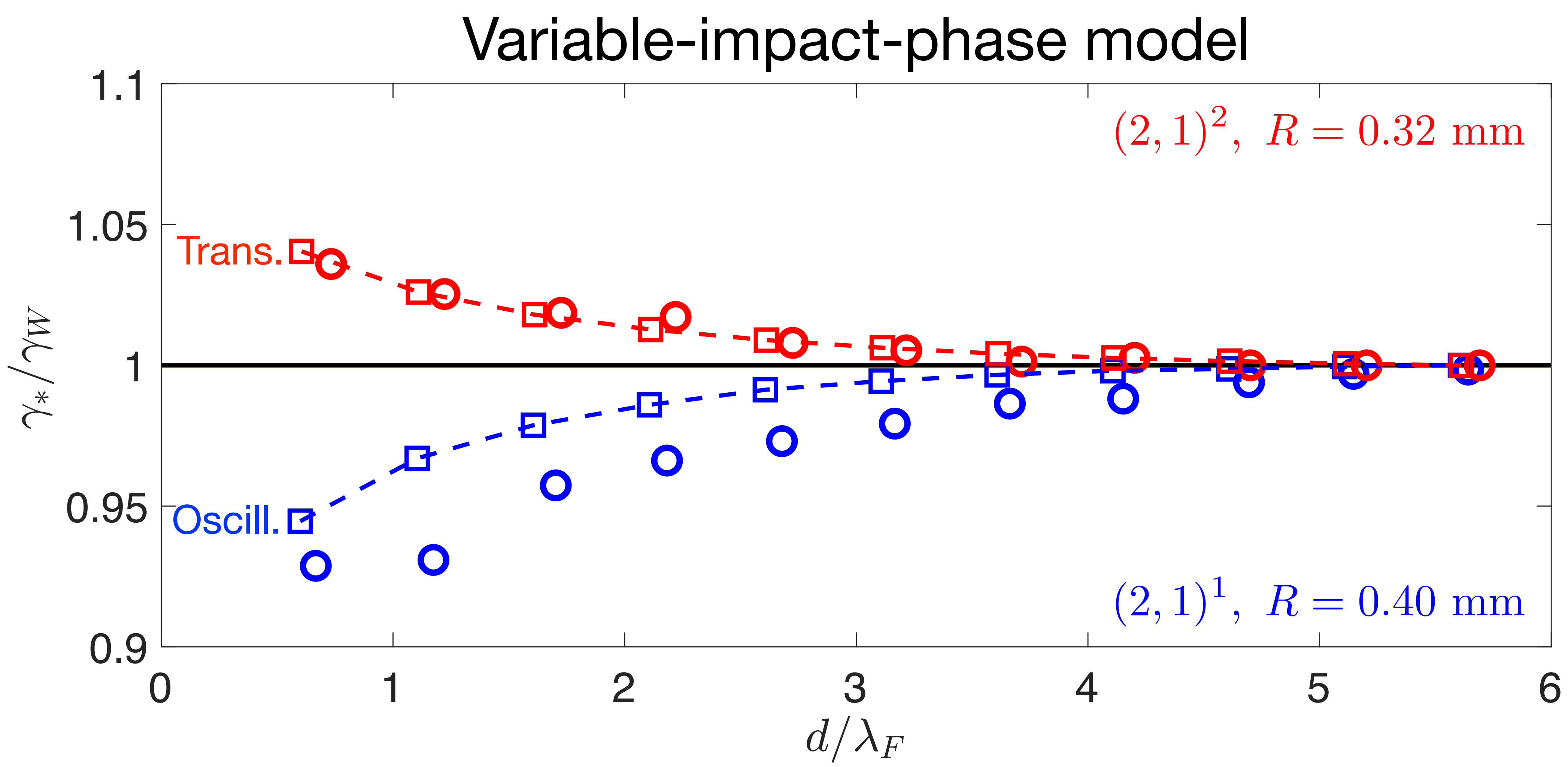

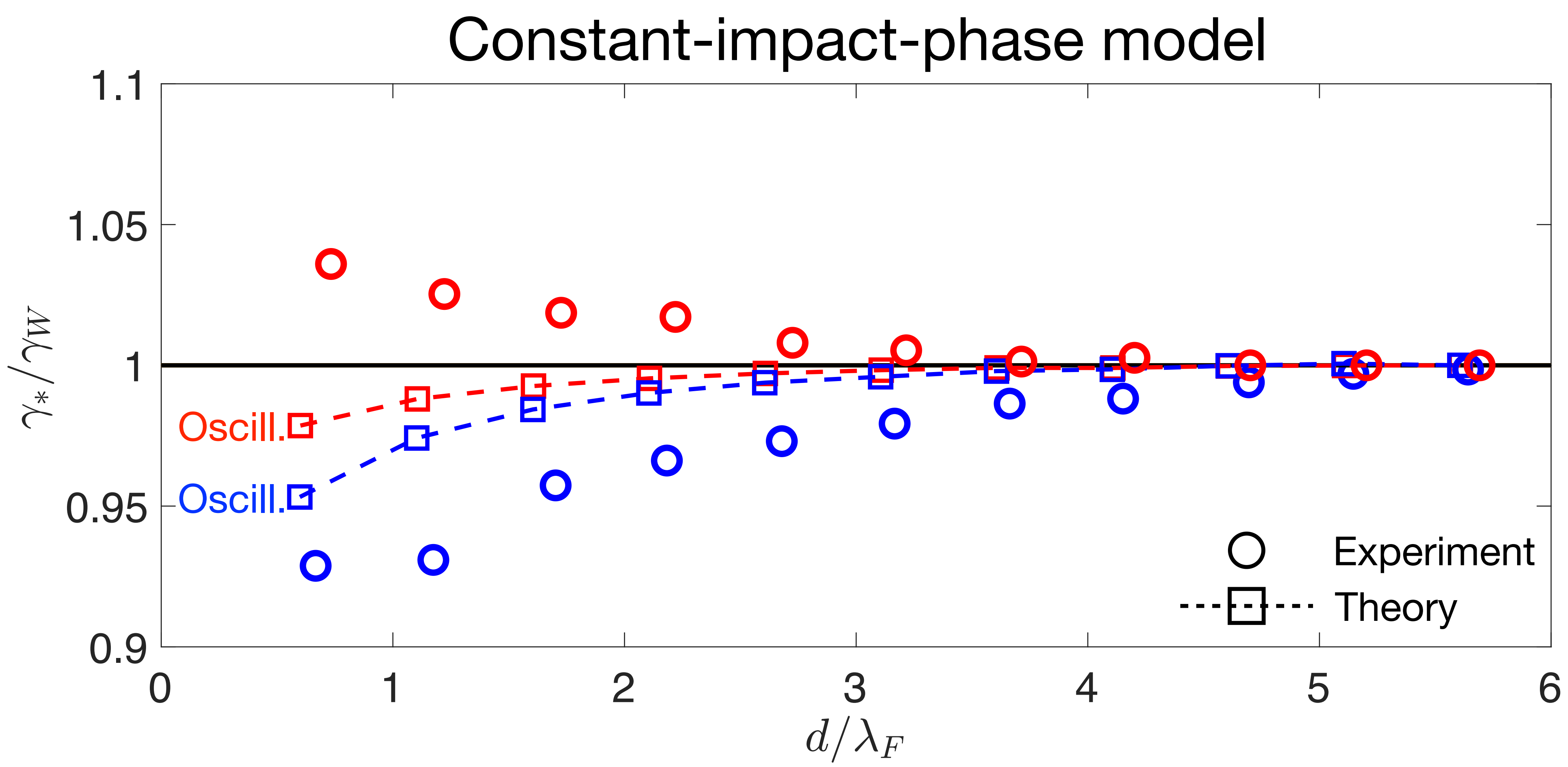

- pairs with smaller inter-drop distance bounce in deeper minimum of neighbor's wavefield
  - $(2,1)^1$: $\mathcal{S}$ and $\mathcal{C}$ increase with decreasing wave amplitude $\longrightarrow$ **destabilization**
  - $(2,1)^2$: $\mathcal{S} \approx 1,\ \mathcal{C}$ decreases with decreasing wave amplitude $\longrightarrow$ **stabilization**

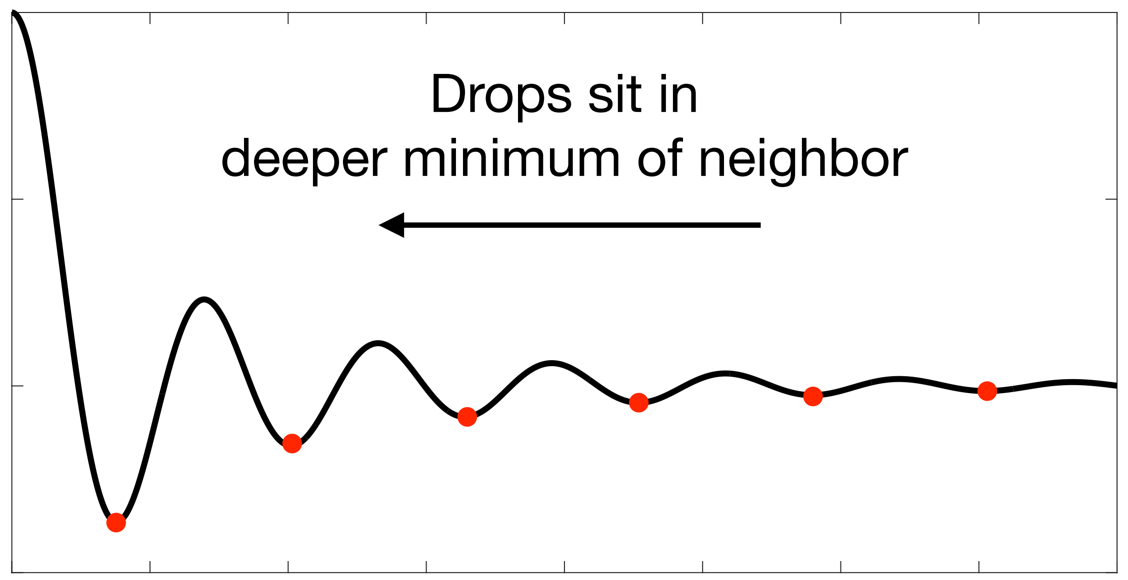

$\mathcal{S}$: governs wave amplitude
$\mathcal{C}$: governs horizontal wave force

The stability of droplet rings

J. Fluid Mech. (2020), vol. 903, A49. © The Author(s), 2020. 903 A49-1
Published by Cambridge University Press
doi: 10.1017/jfm.2020.648

Free rings of bouncing droplets: stability and dynamics

Miles M. P. Couchman[1] and John W. M. Bush[1,†]

[1]Department of Mathematics, Massachusetts Institute of Technology, Cambridge, MA 02139, USA

Vortex arrays

Droplet rings exhibit certain features of vortex arrays in various fields.

- Superfluid helium

  Havelock 1931; Yarmchuk and Gordon 1979; Aref *et al*. 2002; Crowdy 2003; Celli *et al*. 2011

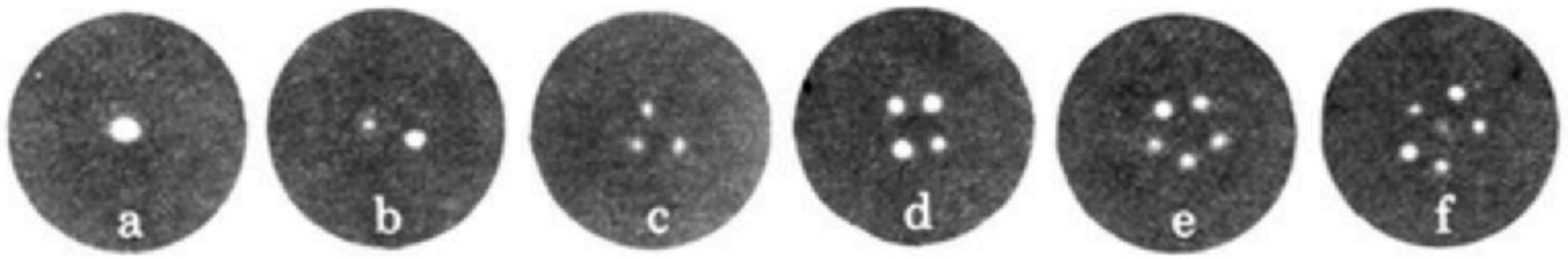

- Hurricane eyewalls

  Kossin and Schubert 2001, 2004

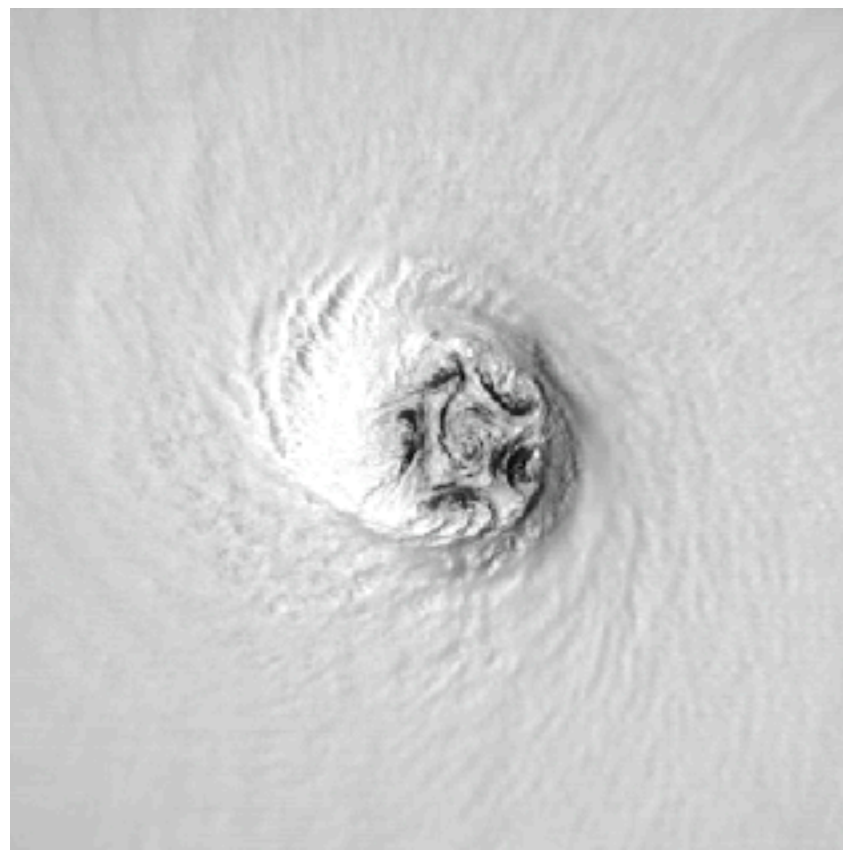

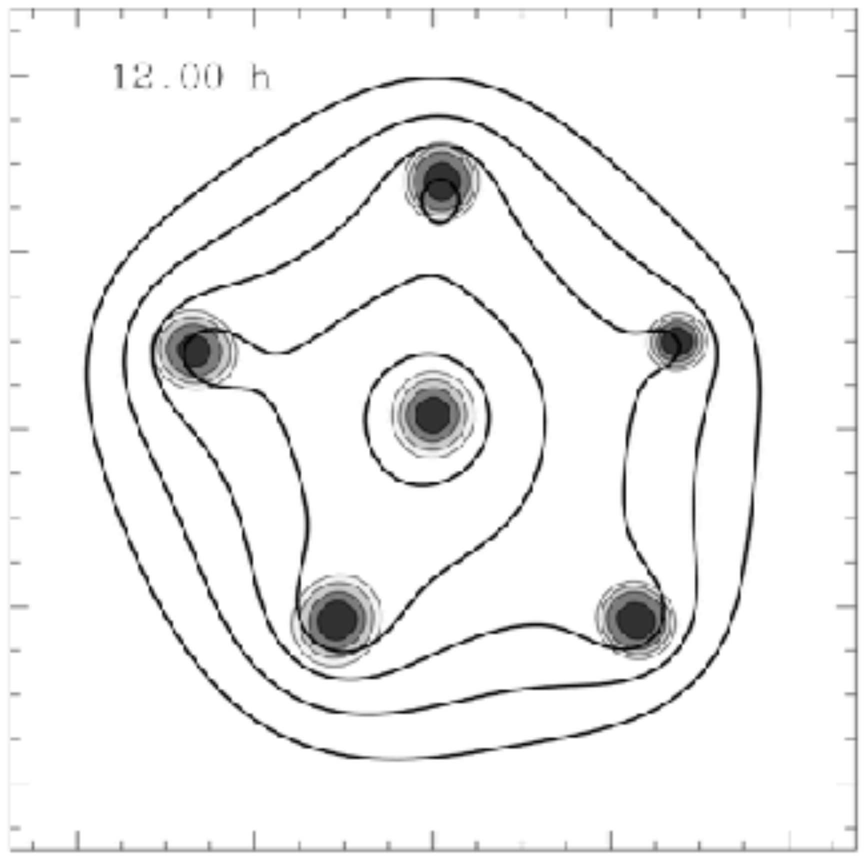

- Magnetized plasmas

  Durkin and Fajans 2000

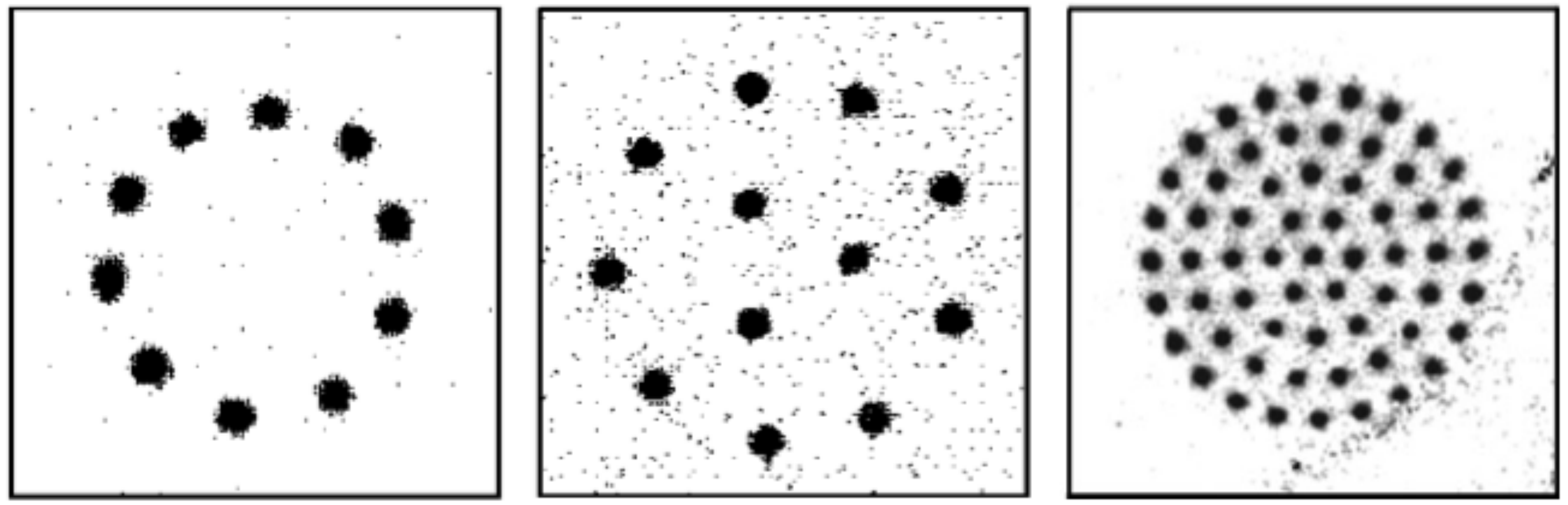

- Bose-Einstein condensates

  Abo-Shaeer *et al*. 2001; Kolokolnikov *et al*. 2014

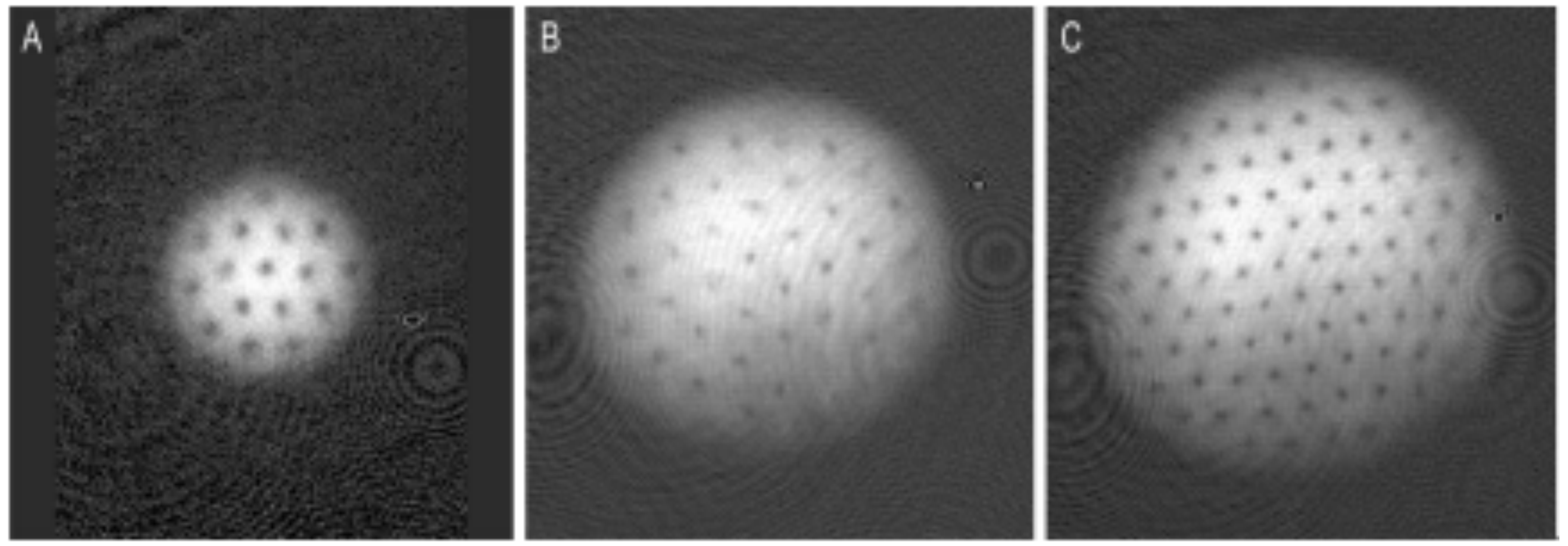

Experiments

- identically sized drops used to form stationary rings at low vibrational acceleration, γ
- rings characterized by radius r_0, drop number N, and whether neighbouring drops are bouncing in-phase or out-of-phase

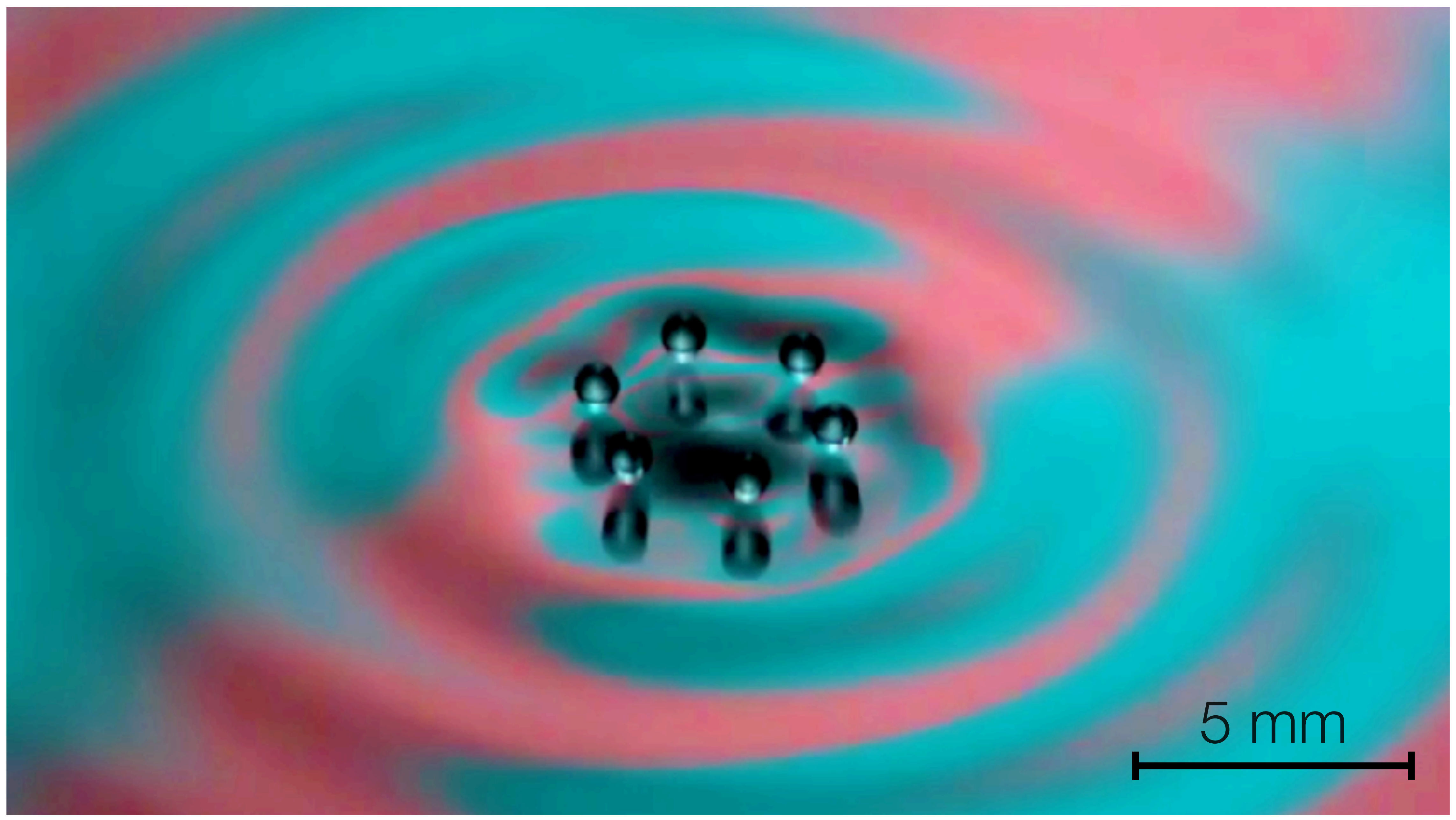

- gradually increase γ and observe how rings destabilize

Ring experiments

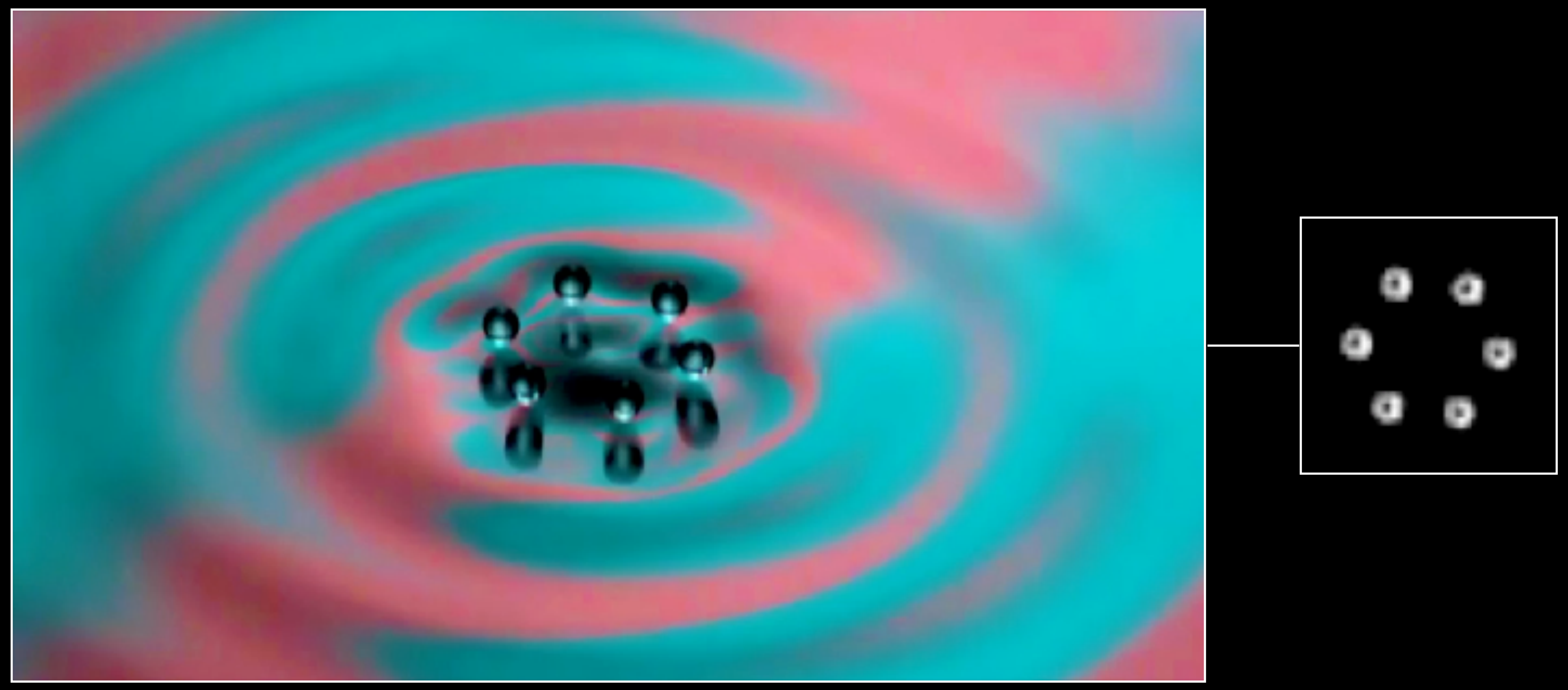

- At low vibrational acceleration, create stable ring
- Drops bounce in minima of wavefield produced by other drops, resulting in a discrete set of possible radii

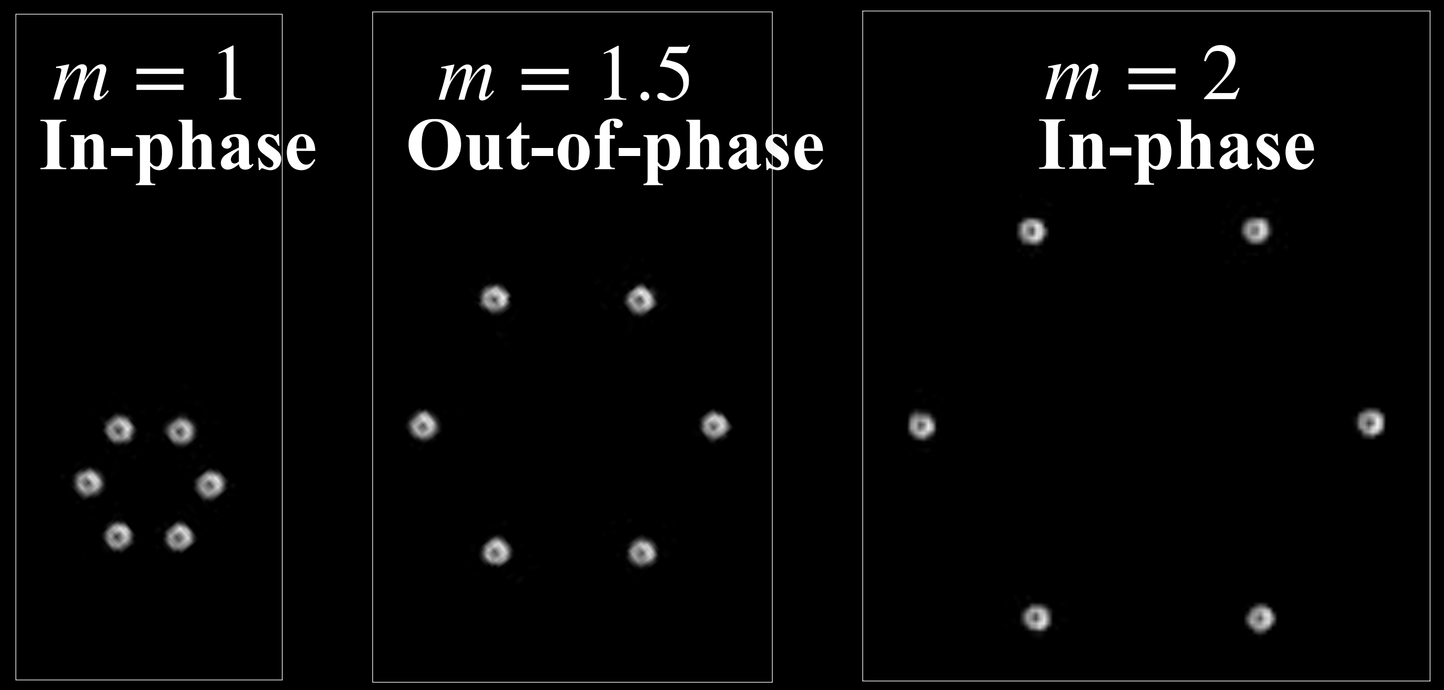

- Gradually increase γ and observe how the ring destabilizes

Instabilities of Tightly Bound Rings $(m = 1)$

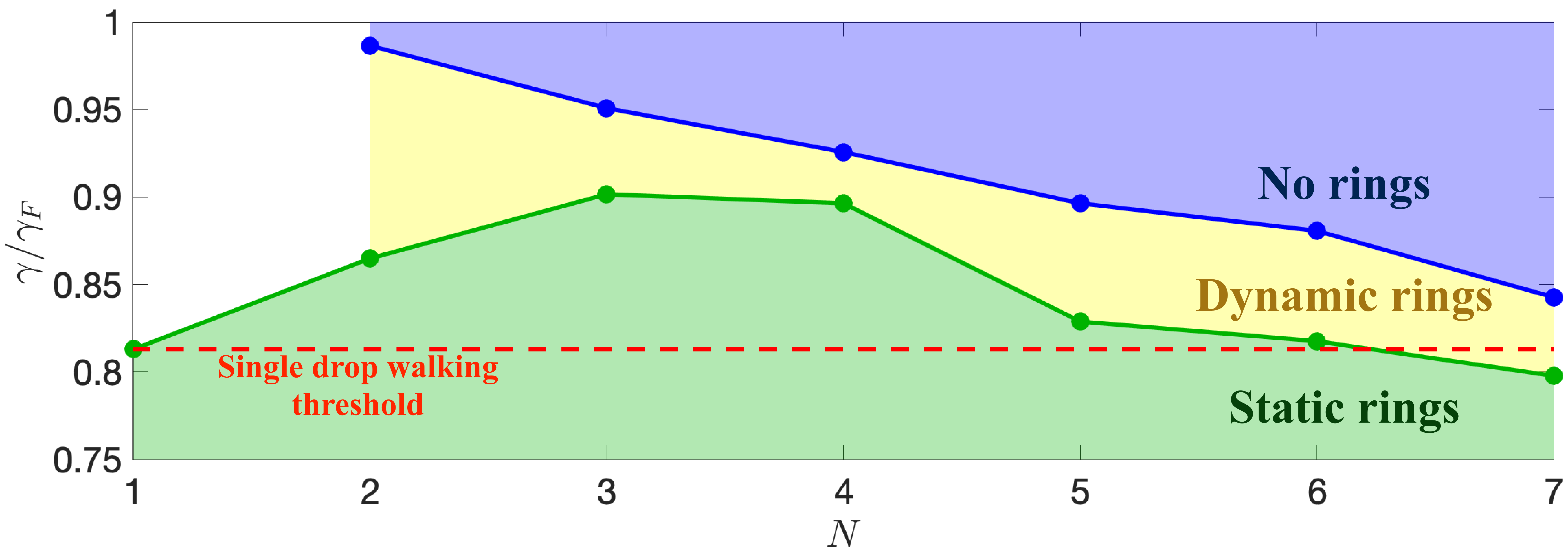

Initial Instability